THE UNIVERSITY *of* EDINBURGH

Edinburgh Research Explorer

Enhancer decommissioning by Snail1-induced competitive displacement of TCF7L2 and down-regulation of transcriptional activators results in EPHB2 silencing

OPEN ACCESS

Accepted Manuscript

Enhancer decommissioning by Snail1-induced competitive displacement of TCF7L2 and down-regulation of transcriptional activators results in EPHB2 silencing

Oskar Schnappauf, Sven Beyes, Annika Dertmann, Vivien Freihen, Patrick Frey, Sabine Jägle, Katja Rose, Tom Michoel, Rudolf Grosschedl, Andreas Hecht

Please cite this article as: Oskar Schnappauf, Sven Beyes, Annika Dertmann, Vivien Freihen, Patrick Frey, Sabine Jägle, Katja Rose, Tom Michoel, Rudolf Grosschedl, Andreas Hecht, Enhancer decommissioning by Snail1-induced competitive displacement of TCF7L2 and down-regulation of transcriptional activators results in EPHB2 silencing, *BBA - Gene Regulatory Mechanisms* (2016), doi: 10.1016/j.bbagrm.2016.08.002

Enhancer decommissioning by Snail1-induced competitive displacement of TCF7L2 and down-regulation of transcriptional activators results in EPHB2 silencing

Oskar Schnappauf[1,2,3], Sven Beyes[1,3], Annika Dertmann[1], Vivien Freihen[1,3], Patrick Frey[1], Sabine Jägle[1], Katja Rose[1], Tom Michoel[4], Rudolf Grosschedl[2], Andreas Hecht[1,3,5,#]

[1] Institute of Molecular Medicine and Cell Research, Faculty of Medicine, University of Freiburg, Stefan-Meier-Str. 17, D-79104 Freiburg, Germany

[2] Department of Cellular and Molecular Immunology, Max Planck Institute of Immunobiology and Epigenetics, Stübeweg 51, D-79108 Freiburg, Germany

[3] Faculty of Biology, University of Freiburg, Schänzlestrasse 1, D-79104 Freiburg, Germany

[4] The Roslin Institute, The University of Edinburgh, Easter Bush, Midlothian EH25 9RG, Scotland, UK

[5] BIOSS Centre for Biological Signalling Studies, Schänzlestrasse 18, D-79104 Freiburg, Germany

[#]corresponding author:

Andreas Hecht

Institute of Molecular Medicine and Cell Research

Albert-Ludwigs-University Freiburg

Stefan-Meier-Str. 17

D-79104 Freiburg, Germany

Phone:+49-761-203 9608

FAX: +49-761-203 9602

e-mail: andreas.hecht@mol-med.uni-freiburg.de

Abstract

Transcriptional silencing is a major cause for the inactivation of tumor suppressor genes, however, the underlying mechanisms are only poorly understood. The *EPHB2* gene encodes a receptor tyrosine kinase that controls epithelial cell migration and allocation in intestinal crypts. Through its ability to restrict cell spreading, EPHB2 functions as a tumor suppressor in colorectal cancer whose expression is frequently lost as tumors progress to the carcinoma stage. Previously we reported that *EPHB2* expression depends on a transcriptional enhancer whose activity is diminished in *EPHB2* non-expressing cells. Here we investigated the mechanisms that lead to *EPHB2* enhancer inactivation. We show that expression of *EPHB2* and *SNAIL1* - an inducer of epithelial-mesenchymal transition (EMT) - is anti-correlated in colorectal cancer cell lines and tumors. In a cellular model of Snail1-induced EMT, we observe that features of active chromatin at the *EPHB2* enhancer are diminished upon expression of murine Snail1. We identify the transcription factors FOXA1, MYB, CDX2 and TCF7L2 as *EPHB2* enhancer factors and demonstrate that Snail1 indirectly inactivates the *EPHB2* enhancer by downregulation of *FOXA1* and *MYB*. In addition, Snail1 induces the expression of Lymphoid enhancer factor 1 (LEF1) which competitively displaces TCF7L2 from the *EPHB2* enhancer. In contrast to TCF7L2, however, LEF1 appears to repress the *EPHB2* enhancer. Our findings underscore the importance of transcriptional enhancers for gene regulation under physiological and pathological conditions and show that SNAIL1 employs a combinatorial mechanism to inactivate the *EPHB2* enhancer based on activator deprivation and competitive displacement of transcription factors.

Keywords

2

Abbreviations:

cDNA: complementary DNA

ChIP: chromatin immunoprecipitation

CRC: colorectal cancer

DHS: DNase I hypersensitive sites

Dox: doxycycline

ECR: evolutionary conserved region

EMSA: electrophoretic mobility shift assay

EMT: epithelial-mesenchymal transition

FAIRE: formaldehyde-assisted isolation of regulatory elements

HA: hemagglutinin

HUVEC: human umbilical vein endothelial cells

LEF: lymphoid enhancer factor

qPCR: quantitative PCR

qRT-PCR: quantitative reverse transcriptase PCR

RT-PCR: reverse transcriptase PCR

SEM: standard error of the mean

TCF: T-cell factor

TUB: TUBULIN

TSS: transcriptional start site

WT: wild-type

1. Introduction

Transcriptional enhancers are defined as *cis*-regulatory DNA elements that increase the activity of homologous and heterologous promoters independently of distance and orientation (reviewed in: [1]). Enhancer DNA contains clusters of transcription factor binding sites and provides a platform for the assembly of multi-component regulatory protein complexes that increase the activity of a linked promoter by various mechanisms, for example by eliciting chromatin structural changes, by recruitment of RNA polymerase II, or by direct promoter communication through the MEDIATOR complex [1]. Enhancers exist in different functional states that are distinguished by characteristic structural features. Inactive or latent enhancers resemble bulk chromatin whereas active enhancers are nucleosome-free or associated with specific histone variants and bound by transcriptional regulators. Nucleosomes flanking active enhancers show higher ratios of the H3K4me1/2 and H3K4me3 marks compared to promoter regions, and are enriched for the H3K27ac mark that is replaced by H3K27me3 at poised enhancers [1]. These distinguishing structural characteristics allow for enhancer functional states to be experimentally probed by DNase I hypersensitive site (DHS) mapping, formaldehyde-assisted isolation of regulatory elements (FAIRE) and chromatin immunoprecipitation (ChIP) using antibodies for transcription factors, histones, or histone modifying enzymes such as the acetyltransferases p300/CBP [1]. Transcriptional enhancers play key roles in the spatiotemporal control of gene expression during organismal development. Likewise, the importance of enhancers in disease states and their contribution to the activation of oncogenes and the silencing of tumor suppressors are increasingly recognized [1-5]. In this regard it is of considerable interest to understand how faulty activation or inactivation of transcriptional enhancers is brought about.

EMT denotes the occurrence of profound changes in the cellular phenotype that are observable under various physiological and pathological conditions [6, 7]. Cells undergoing EMT lose the apical-basal polarity as well as the cell-cell and cell-matrix adhesions characteristic of epithelial cells. Instead, they acquire a fibroblast-like morphology with front-to-rear end polarity and gain increased motility and invasive capacities. These phenotypic changes are reflected by massive alterations in gene expression patterns [7]. In recent years, EMT has received significant attention in the area of cancer research. For instance, EMT was proposed to facilitate tumor cell invasion and dissemination, it was implicated in the acquisition of cancer stem cell properties, and it was shown to confer acquired resistance towards apoptosis, radiation and chemotherapy [6-11]. Pathological forms of EMT can be induced by a variety of tumor-cell intrinsic but also environmental signaling cascades all of which ultimately induce the expression of one or several members of the SNAIL, ZEB, and

4

TWIST families of DNA binding proteins [6, 7]. These EMT inducing transcription factors primarily act as transcriptional repressors but can also activate gene expression. Although numerous genes are known that are directly or indirectly regulated by EMT inducers, only very limited mechanistic information exists to explain how changes in gene expression are achieved during EMT.

The *EPHB2* gene encodes a receptor tyrosine kinase that is expressed in the stem cell population located at the base of the crypts of Lieberkühn in the intestinal epithelium [12, 13]. Under physiological conditions, EPHB2 receptor activity has substantial mitogenic effects and additionally controls cell migration and cell positioning along the crypt axis [12, 14]. The ability of EPHB2 to restrict cellular movement is thought to underlie EPHB2 tumor suppressor function in CRC and the loss of *EPHB2* expression seems to facilitate tumor cell invasion [15, 16].

A known regulator of *EPHB2* expression in the intestine is the Wnt/β-catenin pathway [12, 17]. Wnt/β-catenin signaling is of critical importance during development and adult homeostasis of the gastro-intestinal tract [18]. Aberrant Wnt/β-catenin pathway activity also plays a key role throughout all stages of colorectal tumorigenesis [19]. A central aspect of this pathway is the control of the transcriptional co-activator function of β-catenin. Upon pathway activation by ligand/receptor interactions or by mutation of certain pathway components, β-catenin enters the nucleus where it interacts with diverse transcription factors [18]. However, the lion's share of Wnt/β-catenin transcriptional responses is mediated by complexes formed between β-catenin and members of the TCF/LEF family which in humans is comprised of LEF1, TCF7, TCF7L1 and TCF7L2 [20]. Although all TCF/LEF proteins share certain structural similarities including the β-catenin binding domain and the highly conserved HMG-box DNA binding domain, amino acid sequences outside these domains show considerable divergence [20]. As a result, significant functional differences among TCF/LEF proteins exist [21-24].

As a Wnt/β-catenin target gene, *EPHB2* shows a particular, biphasic temporal expression profile in the course of intestinal tumorigenesis. *EPHB2* expression increases in the wake of Wnt/β-catenin pathway hyperactivation at the onset of colorectal tumorigenesis. However, initial upregulation of *EPHB2* is frequently followed by secondary downregulation at the adenoma-carcinoma transition which is in agreement with the known role of *EPHB2* as a tumor suppressor [15, 25-27]. How *EPHB2* expression is silenced and becomes uncoupled from Wnt/β-catenin signaling is not completely understood. Several recent findings prompted us to explore a potential mechanistic link between EMT and enhancer inactivation. For

instance, in a model of SNAIL1-induced EMT, *EPHB2* is subject to late stage downregulation, which argues that *EPHB2* may be indirectly repressed by SNAIL1 [28]. Furthermore, in a previous study we identified a transcriptional enhancer within the *EPHB2* 5'-flanking region [2]. This enhancer displays cell-type-specific activity and loss of enhancer function was observed in *EPHB2* non-expressing CRC cells even in the presence of Wnt/β-catenin pathway activating mutations. This suggested that *EPHB2* enhancer inactivation contributes to *EPHB2* secondary silencing. However, the underlying cause for *EPHB2* enhancer decommissioning and whether SNAIL1 contributes to this remained unknown. We now report that SNAIL1 downregulates the transcription factors MYB and FOXA1, which are required for *EPHB2* enhancer function. Moreover, SNAIL1 induces expression of LEF1, which replaces TCF7L2 at the *EPHB2* enhancer. This switch in occupancy by two functionally different Wnt/β-catenin effectors appears to abrogate Wnt responsiveness of *EPHB2*. Overall, our results provide insights into the molecular workings of *EPHB2* enhancer inactivation during EMT. The observed complexity of this multi-faceted process offers new perspectives for the mechanistic understanding of enhancer decommissioning and might also be pertinent to other models.

2. Materials and methods

2.1. Bioinformatic analyses of microarray gene expression data

For comparative expression analyses of *EPHB2* and *SNAI1/LEF1* in the transcriptomes of human colorectal tumors and cell lines, the normalized microarray datasets GSE14333 (290 colorectal tumor samples) and GSE59875 (155 CRC cell lines) were obtained from The Gene Expression Omnibus Website (http://www.ncbi.nlm.nih.gov/geo/). Absolute gene expression levels were obtained by averaging over multiple probesets for the same gene, and relative expression levels by standardizing each gene to have mean zero and standard deviation one over all samples. Samples were sorted according to highest difference in expression levels between *EPHB2* and *SNAI1/LEF1* and the relative expression values of *EPHB2* and *SNAI1/LEF1* are shown. The pairwise Pearson correlation coefficient between 8 genes of interest was calculated from the same microarray datasets. Genes were clustered in the pairwise correlation matrix using single linkage with Euclidean distance as previously described [2]. To examine the association between the expression of *EPHB2* and either an EMT gene set or the *EPHB2* enhancer factor gene set, we calculated the mean of the absolute expression values for all components of each gene set. Subsequently, the pairwise linear correlation coefficients between the gene set expression value and the absolute expression value of *EPHB2* for each tumor sample or CRC cell line was determined.

2.2. Statistical analysis

The mean of three independent biological replicates with the corresponding standard error of the mean (SEM) was taken in order to represent all quantitative data. In the case of quantitative PCR analyses and luciferase reporter assays, the numerical values for each biological replicate were determined by duplicate measurements (two technical replicates) of a given sample. For calculation of statistical significance an unpaired, two-tailed Student's *t*-test was used unless otherwise indicated. Numbers of asterisks represent statistically significant changes with the following P values: * $P < 0.05$, ** $P < 0.01$, *** $P < 0.001$.

2.3. Identification of evolutionary conserved regions and sequence analyses

Evolutionary conserved regions (ECRs) were identified using the ECR browser (http://ecrbrowser.dcode.org/) [29] which defines regions with at least 70% nucleotide

sequence identity over 100 bp as ECRs. Transcription factor binding sites were determined using MotifMap (http://motifmap.ics.uci.edu) and the JASPAR database (http://jaspar.binf.ku.dk) [30, 31]. DHS and chromosomal regions with high levels of the histone modifications H3K4me1 and H3K27ac in human umbilical vein endothelial cells (HUVEC) were obtained from the UCSC Genome Browser using the Human Feb. 2009 (GRCh37/hg19) Assembly (http://genome.ucsc.edu/) [32].

2.4. Plasmid construction and cloning

To generate luciferase reporter constructs covering portions of the human *EPHB2* upstream region, DNA fragments were amplified by PCR from genomic DNA isolated from LS174T cells and blunt-end cloned into pZERO (Invitrogen/Life Technologies, Darmstadt, Germany). Restriction enzymes SacI and NheI were used to transfer the fragments into the pGL3promoter plasmid (Promega, Heidelberg, Germany) by standard cloning techniques. *EPHB2* upstream fragments with nucleotide sequences corresponding to positions -8398/-8330, -8350/-8272 and -8350/-8330 relative to the transcriptional start site were generated via annealing of equal amounts of complementary oligonucleotides in 1x NEB buffer 2 for 5 min at 95°C followed by 60 min of slow cooling to room temperature. Sequences of the oligonucleotides used are listed in Table 1. Mutagenesis of transcription factor binding sites was performed according to the Stratagene QuikChange^{TM} site-directed mutagenesis protocol. Oligonucleotide primers used are listed in Table 1. Successful mutagenesis was verified by sequencing. The *CDX2* coding region was amplified by PCR using pDONR223-CDX2 as template (kindly provided by the BIOSS Toolbox, Freiburg, Germany) with the following primer pair: 5′-GGATCCGCATGTACGTGAGCTACCTCCTGGACAA-3′ and 5'-TTCGAACTGGGTGACGGTGGGGTTTAGC-3′. The resulting PCR product was cut with BamHI and BstBI and ligated into a derivative of the pCS2+ plasmid [33] providing the coding region for a hemagglutinin (HA)-tag. The MYB coding region (containing an HA-tag) was released from pCI-neo-MYB (kindly provided by K.-H. Klempnauer, University of Münster, Germany) with XhoI and XbaI and ligated into pCS2+. Expression vectors for human TCF7L2-E and mouse Lef1 were previously described [34]. For the generation of stably transduced cell lines for Dox-inducible expression of Lef1-HA, the coding region for Lef1-HA was cloned into the pRetroX-tight-Pur vector (Clontech, Saint-Germain-en-Laye, France) by standard cloning techniques. For the generation of stably transduced cell lines for Dox-inducible expression of SNAIL2-HA, the coding region for SNAIL2-HA was cut out from pCS2+SNAIL2-HA and cloned into the pRetroX-tight-Pur vector [28]. The stably transduced cell lines for Dox-inducible expression of ZEB1-HA were generated by releasing the coding

region of human ZEB1-HA with NotI and Bsp120I from the plasmid pTET Bsr HA-ZEB1-IRES berry [35] (kindly provided by T. Brummer, University of Freiburg, Germany) and cloning into the pRetroX-tight-Pur vector (Clontech, Saint-Germain-en-Laye, France).

2.5. Cell culture

The CRC cell lines LS174T (CLS #300392) and SW403 (CLS #300350) were obtained from the Cell Line Service culture collection (DKFZ, Heidelberg, Germany). SW480 and HCT116 cell lines were obtained from the Max Planck Institute of Immunobiology and Epigenetics, Freiburg, Germany. Identity of the cell lines was confirmed by a multiplex human cell line authentication test (Multiplexion, Immenstaad, Germany). Cells were cultured as previously described [25]. To generate the stable Lef1-HA expression cell line, retroviral infection with pRetroX-tight-Pur-based vectors was used as described [23]. As recipients, LS174T cells stably transfected with the pN1pßactin-rtTA^{2S}-M2-IRES-EGFP plasmid were used [36]. LS174T cells transduced with a Dox-inducible Snail1-HA retroviral vector were previously described [28]. To induce protein expression in stable cell lines, cells were treated with 0.1 µg/ml Dox or 1 µg/ml Dox for the indicated time periods as described in the figure legends.

2.6. Luciferase reporter assays

For luciferase reporter assays, 1 x 10^5 LS174T, SW480 and HCT116 cells or 2 x 10^5 SW403 cells per well were seeded in 24-well plates and transfected with the FuGENE6 reagent (Promega, Heidelberg, Germany) according to the manufacturer's protocol. The cells received a mixture of 10 ng of the Renilla luciferase expression vector pRL-CMV (Promega, Heidelberg, Germany) and 250 ng of pGL3promoter plasmid containing the indicated *EPHB2* fragments. Cell lysates were prepared and reporter activity was determined 48 h after transfection as described [23]. Renilla luciferase activity was used for normalization.

2.7. RNA isolation, cDNA synthesis and quantitative reverse transcriptase-PCR

Total RNA was isolated using the peqGOLD total RNA Kit (PeqLab, Erlangen, Germany). Complementary DNA (cDNA) synthesis and reverse transcriptase (RT)-PCR were performed as previously described [23]. For cDNA synthesis, 500 ng of total RNA was used as template and oligo-dT oligonucleotides served as primers. Quantitative RT-PCR (qRT-PCR) was

performed with the CFX-96 multicolor real-time PCR detection system (BioRad, Munich, Germany) using SYBR green reaction mix (PeqLab, Erlangen, Germany). A cDNA amount equivalent to 20 ng of total RNA was used as template. Values shown represent expression of the genes-of-interest relative to GAPDH. Primers are listed in Table 1.

2.8. Western blotting and immunodetection

Protein expression levels of CDX2, FOXA1 and MYB were determined using nuclear extracts. For this, cells from three 15 cm dishes were used. After washing with ice-cold PBS, cells were collected, pooled, and transferred to 15 ml tubes. Cells were centrifuged at 500 x g and 4°C for 5 min. Then, the cell pellet was resuspended in a fivefold volume of hypotonic swelling buffer [10 mM Hepes/KOH pH 7.9, 0.75 mM spermidine, 0.15 mM spermin, 0.1 mM EDTA, 0.1 mM EGTA, 10 mM KCl, Complete protease inhibitor (Roche, Mannheim, Germany), 1 mM DTT, 0.5 mM PMSF] and incubated on ice for 10 min upon which cells were mechanically lysed by 15 strokes in a dounce homogenizer with tight-fitting pestle. Afterwards, 1 volume of sucrose restore buffer [8 volumes 75% (wt/vol) sucrose combined with 1 volume 10 x salt buffer (500 mM Hepes/KOH pH 7.9, 7.5 mM spermidine, 1.5 mM spermin, 2 mM EDTA, 1 mM EGTA, 100 mM KCl, Complete protease inhibitor, 1 mM DTT)] was added, and nuclei were pelleted by centrifugation at 4°C and 4,600 x g for 5 min. The supernatant was discarded, and the nuclei were resuspended in nuclei extraction buffer [20 mM Hepes/KOH pH 7.9, 0.75 mM spermidine, 0.15 mM spermin, 0.2 mM EDTA, 0.1 mM EGTA, 25% (vol/vol) glycerin, 400 mM KCl, Complete protease inhibitor, 1 mM DTT, 0.5 mM PMSF] at 4°C for 30 min with constant gentle agitation. The nuclear extract was cleared by centrifugation at 110,000 x g and 4°C for 30 min and then stored at -80°C. For the detection of SNAIL1, EPHB2, TCF7L2 and LEF1 whole-cell lysates were prepared by lysing cells in IPN-150 (50 mM Tris/HCl pH 7.6, 150 mM NaCl, 5 mM $MgCl_2$, 0.1% Nonidet P-40, Complete protease inhibitor, 1 mM DTT) for 30 min on ice. Thereafter, cell lysates were cleared by centrifugation at 16,000 x g and 4°C for 10 min. Protein concentration was determined using the DC Protein Detection Kit (BioRad, Munich, Germany). Proteins were separated by SDS-polyacrylamide gel electrophoresis and transferred on nitrocellulose membranes.

For immunodetection, the following antibodies were used: Goat polyclonal anti-EPHB2 (1:1,000, AF467; R&D Systems, Minneapolis, USA), mouse monoclonal anti-α-TUBULIN (1:10,000, T9026; Sigma-Aldrich, St. Louis, USA), mouse monoclonal anti-GSK3β (1:1,000, 610201; BD Biosciences, Franklin Lakes, USA), rat monoclonal anti-HA (1:1,000, 3F10; Roche, Mannheim, Germany), mouse monoclonal anti-LEF1 (1:1,000, sc-81470,

Santa Cruz, Heidelberg, Germany), rabbit monoclonal anti-TCF7L2 (1:1,000, 2565; Cell Signaling Technology, Cambridge, UK), goat polyclonal anti-FOXA1 (1:1,000, ab5089, Abcam, Cambridge, UK), rabbit monoclonal anti-v-MYB and c-MYB (1:1,000, ab45150, Abcam, Cambridge, UK), rabbit monoclonal anti-CDX2 (1:1,000, D11D10, Cell Signaling Technology, Cambridge, UK), rabbit polyclonal anti-POL2 (1:1,000, sc-899, Santa Cruz, Heidelberg, Germany), rabbit polyclonal anti-ZEB1 (1:2,000, HPA027524, Sigma-Aldrich, St. Louis, USA), rabbit monoclonal anti-SNAIL2 (1:1,000, 5% BSA, C19G7/#9585, Cell Signaling Technology, Cambridge, UK), rabbit monoclonal anti-Snail1 (1:1,000, 5% BSA, C15D3/#3879, Cell Signaling Technology, Cambridge, UK). Visualization of antibody:antigen complexes was performed as previously described [24].

2.9. Electrophoretic mobility shift assay (EMSA)

EMSAs were used to study DNA binding of transcription factors to the *EPHB2* minimal enhancer fragment *in vitro*. Proteins of interest were transcribed and translated *in vitro* using the TNT SP6 high-yield wheat-germ protein expression system with 2.5 µg of the plasmid DNA in 25 µl reactions at 25°C for 120 min (Promega, Heidelberg, Germany). Protein expression was confirmed by Western blot. DNA probes for EMSA were generated by PCR with biotinylated primers using wild type or mutated versions of the *EPHB2* -8398/-8272 enhancer subfragment as DNA template. Sequence information for the oligonucleotides used is given in Table 1. 10 fmol of the biotinylated probe were combined with equal amounts of the protein of interest, 60 µg of bovine serum albumin, 1 µg poly(dI:dC) and incubated in EMSA-buffer (20 mM Hepes/KOH pH 7.9, 75 mM NaCl, 2 mM $MgCl_2$, Complete protease inhibitor, 1 mM DTT) for 30 min on ice (total volume: 20 µl). For the competitive EMSAs, only 1 fMol of biotinylated probes were used. Binding reactions were loaded onto 6% (wt/vol) polyacrylamide gels with 0.5 x Tris-borate-EDTA running buffer to separate the complexes. For further processing, the chemiluminescent nucleic acid detection module (Thermo Fisher Scientific, Dreieich, Germany) was used according to the manufacturer's protocol.

2.10. Formaldehyde-assisted isolation of regulatory elements (FAIRE)

FAIRE was used to enrich for nucleosome depleted DNA and was performed as previously described [2]. The cells used for the experiments were crosslinked with 1% formaldehyde for 7 min or were left untreated as reference material. Sonification was performed with 300 µl aliquots of the sample for 20 cycles with 30 s on/30 s off (high amplitude) in a Bioruptor Plus

(Diagenode, Denville, USA) producing DNA fragments between 250 and 750 bp in length. For quantitative PCR (qPCR), 40 ng DNA was used that had been recovered from crosslinked cells and non-crosslinked reference material. Data calculation was conducted as previously described [23]. Primer sequences are listed in Table 1.

2.11. Chromatin immunoprecipitation

Chromatin immunoprecipitation (ChIP) was performed as described [2]. Briefly, cells were crosslinked with 1% formaldehyde, chromatin was isolated and sheared by sonication. For precipitations with the anti-HA antibody, 200 µg chromatin were used. In all other cases of antibodies 100 µg chromatin were used. The amounts of antibodies employed for ChIP were as follows: 1 µg of rabbit polyclonal anti-HA (ab9110; Abcam, Cambridge, UK), 2 µg of rabbit polyclonal anti-H3 (ab1791; Abcam, Cambridge, UK), 2 µg of rabbit polyclonal anti-H3K4me1 (pAb-037–050; Diagenode, Denville, USA), 2 µg of rabbit polyclonal anti-H3K27ac (ab4729; Abcam, Cambridge, UK), 2 µg of goat polyclonal anti-TCF7L2 (N-20, sc-8631; Santa Cruz, Heidelberg, Germany), 2 µg of mouse monoclonal anti-LEF1 (sc-81470, Santa Cruz, Heidelberg, Germany), 3 µg of goat polyclonal anti-FOXA1 (ab5089, Abcam, Cambridge, UK), 2 µg of rabbit monoclonal anti-v-MYB and c-MYB (ab45150, Abcam, Cambridge, UK), 2 µg of goat polyclonal anti-β-catenin (AF1329, R&D Systems, Minneapolis, USA). qPCR was performed as described above using 1 µl of precipitated DNA and 2% of the input material as template with primers listed in Table 1. Data were calculated as percent input relative to H3 (H3K27ac, H3K4me1) or as percent input (transcription factor ChIPs).

3. Results

3.1. Expression of Snail1-HA diminishes features of active chromatin at the EPHB2 -8.4 kb enhancer

There is a statistically significant negative correlation between the expression of *EPHB2* and the average expression of a gene set consisting of EMT inducers (including *SNAI1*) and markers of mesenchymal cells (*FN1*, *VIM*) in the transcriptomes of 290 colorectal tumor samples (GSE14333; Fig. S1A). A trend of anti-correlated expression in colorectal tumor samples and in a cohort of 155 CRC cell lines (GSE59857) can also de detected by the pairwise analysis of *EPHB2* and *SNAI1* expression levels (Fig. S1B). Typically, samples with high *EPHB2* levels show low expression of *SNAI1* and vice versa. The inverse relationship between *EPHB2* and *SNAI1* expression can also be seen at the mRNA and protein levels in the LS174T, SW480, HCT116 and SW403 CRC cell lines (Fig. S1C,D). Furthermore, Dox-induced expression of mouse Snail1-HA in LS174T CRC cells leads to the downregulation of *EPHB2* over a time period of 96 h (Fig. S1E,F).

Overall, these observations strongly suggest that *EPHB2* is negatively regulated by SNAIL1 in CRC. On the other hand, we previously implicated a cell-type-specific enhancer element located at -8.4 kb upstream of the *EPHB2* transcriptional start site (TSS) in the differential expression of *EPHB2* in CRC cells [2]. However, it is not known whether this enhancer is the sole element involved in pathological *EPHB2* silencing and whether the enhancer is targeted by SNAIL1. As a first step to address these questions we therefore performed bioinformatic analyses to systematically screen the *EPHB2* 5'-region for the presence of potential regulatory elements. Thereby, a large number of evolutionary conserved DNA sequence blocks were identified that could represent regulatory elements (Fig. 1A). To further pinpoint potential control elements we queried the ENCODE data base (http://genome.ucsc.edu/; Human Feb. 2009 (GRCh37/hg19) Assembly) as an additional source of information. This analysis indicated the occurrence of DNase I hypersensitive sites (DHS) in chromatin of HUVEC cells around -8.0 kb, -6.0 kb, and close to the TSS. The general enhancer mark H3K4me1 appeared to be enriched around -8.0 kb and -6.0 kb (Fig. 1A). The ENCODE data furthermore suggested an enrichment of the histone modification H3K27ac that specifies active enhancers and promoter regions, around -8.0 kb and close to the TSS. In summary, the bioinformatic screen identified three candidate regulatory regions: the already known enhancer region, the region around -6.0 kb, and distal promoter elements.

As a next step, we performed FAIRE experiments with CRC cell lines and scanned the *EPHB2* 5'-region for differences in chromatin structure that might be linked to differential *EPHB2* expression (Fig. S2A,B). In agreement with the results described above, we observed an elevated FAIRE signal at -8.4 kb, -6.2 kb, and close to the TSS. However, only the -8.4 kb region showed a reduction of the FAIRE signal in SW480 and HCT116 cells where *EPHB2* is not expressed. ChIP experiments further confirmed that *EPHB2* expression states are reflected by differences in the association of the *EPHB2* -8.4 kb region with histone H3, H3K4me1 and H3K27ac (Fig. S2C). Interestingly, when we analyzed the same chromatin features in LS174T cells with Dox-inducible expression of Snail1-HA before and after Dox treatment, we observed a clear shift from an active enhancer state to a more inactive conformation, as indicated by a diminished FAIRE signal around -8.4 kb. (Fig. 1B). No other statistically significant chromatin structural changes within the *EPHB2* 5'-region were observed. ChIP experiments with antibodies against H3 additionally confirmed a more condensed chromatin state of the *EPHB2* -8.4 kb region upon Snail1-HA induction (Fig. 1C). Furthermore, the levels of the more general enhancer modification H3K4me1 seem to be reduced upon Snail1-HA as well. ChIP analyses also showed a clear reduction in the levels of the active enhancer mark H3K27ac (Fig. 1C).

We also performed luciferase reporter gene assays to functionally assess the regulatory potential of the *EPHB2* -6.2 kb region. For comparison, constructs with the *EPHB2* -8.4 kb enhancer and a fragment that covers an extended block of evolutionary conserved sequences around -11 kb were included in the experiments (Fig. S3). The results of the reporter gene assays confirmed the cell-type-specific enhancer function of the *EPHB2* -8.4 kb region. In contrast, neither the -11 kb fragment nor the -6.2 kb region were able to stimulate or repress luciferase reporter activity in CRC cells that differ with respect to *EPHB2* expression (Fig. S3). Thus, the results obtained up to this point indicate that the cell-type-specific enhancer at -8.4 kb within the *EPHB2* locus that is active only in the *EPHB2* expressing CRC cell lines is also likely to be the target for decommissioning by the EMT inducer SNAIL1.

3.2. EPHB2 enhancer activity depends on CDX2, TCF7L2, FOXA1 *and* MYB

To learn more about the regulation of the *EPHB2* -8.4 kb enhancer region, we sought to identify the smallest enhancer DNA fragment that still exhibited differential activity in CRC cell lines. Therefore, luciferase reporter assays with different fragments of the *EPHB2* enhancer region were performed in four CRC cell lines that differ in their *EPHB2* expression

14

(Figs. 2 and S4). The longest fragment tested completely covered the described region with elevated levels of H3K4me1, H3K27ac and DHS (Figs. 2 and S4, fragment 1). The analysis of this fragment in luciferase reporter assays showed elevated luciferase expression only in LS174T cells and not in SW480, HCT116 and SW403. To narrow down the size of the enhancer, the fragment was further split into two overlapping subfragments (Figs. 2 and S4, fragments 2 and 3). Interestingly, both *EPHB2* enhancer fragments 2 and 3 were able to increase luciferase expression in LS174T and SW403 CRC cell lines and not in SW480 and HCT116, thereby confirming the suggested cell-type-specificity of the *EPHB2* enhancer fragment. The overlap of these two fragments exhibited the described cell-type-specificity as well (Figs. 2 and S4, fragment 4). Further reduction in fragment size showed that the 126 bp fragment 5 was also able to drive increased luciferase expression in LS174T and SW403 CRC cell lines but not in SW480 and HCT116 cells at levels comparable to those of fragments 1-4 (Figs. 2 and S4, fragment 5). The 78 bp fragment 7 was also endowed with cell-type-specific enhancer activity but appeared to be somewhat less active than fragment 5, especially in LS174T cells (Figs. 2 and S4, fragment 7). In contrast, fragments 6 and 8 had a much reduced, albeit statistically significant potential to stimulate luciferase reporter activity (fragment 6: LS174T and SW403 cells; fragment 8: LS174T cells) and even exhibited some cell-type-specificity (Figs. 2 and S4). These findings led us to conclude that the minimal cell-type-specific enhancer fragment of the *EPHB2* -8.4 kb enhancer region can be confined to fragment 5, covering *EPHB2* upstream sequences -8398/-8272*.*

Next, we aimed to identify potential binding sites for transcription factors within the *EPHB2* minimal enhancer fragment -8398/-8272 using different online tools for transcription factor binding motif prediction [30, 31]. In combination with additional manual inspection, this led to the identification of putative binding sites for several transcription factors with well known roles in the development and maintenance of intestinal epithelial stem cells, namely CDX2, MYB, members of the TCF/LEF family, and members of the FOX transcription factor family (Fig. 3A) [37-41]. Single, discrete binding motifs for CDX2 and TCF/LEF proteins were predicted, however, single but overlapping FOX and MYB binding motifs were found.

As a first step towards testing the importance of these motifs for *EPHB2* enhancer function, we performed EMSAs with recombinant CDX2, TCF7L2, FOXA1 and MYB using the *EPHB2* fragment -8398/-8272 as probe. To demonstrate binding specificity, EMSAs with probes harboring mutated versions of the transcription factor binding motifs were performed in parallel (Fig. 3B). Both TCF7L2 and MYB formed a sole protein::DNA complex with the wild-type (WT) *EPHB2* enhancer probe. These complexes completely disappeared when their presumptive binding sites were mutated (Figure 3B,C). Although the *in silico* analyses

15

had predicted only a single binding site each for CDX2 and FOXA1, both factors formed two DNA::protein complexes with the *EPHB2* enhancer probe (Fig. 3C). This could be alternatively explained by the presence of additional, cryptic binding sites that could not be identified by the *in silico* search, or by the formation of protein multimers independently of the presence of a second binding site within the *EPHB2* enhancer sequences. In support of the latter possibility we observed that mutation of the single predicted CDX2 binding motif nonetheless abolished formation of both CDX2::DNA complexes. Likewise, formation of both FOXA1::DNA complexes was simultaneously impaired when just the one predicted FOX binding site was mutated. Altogether we conclude that CDX2, TCF7L2, FOXA1, and MYB can specifically interact with *EPHB2* enhancer sequences *in vitro*.

We were interested in the functional importance of the identified transcription factor binding sites. To this end we performed luciferase reporter assays with WT and mutated versions of the *EPHB2* -8398/-8272 enhancer construct in LS174T cells. As expected, we observed a clear increase in luciferase expression in the presence of the WT enhancer sequences (Fig. 3D). Enhancer activity was reduced by 77% when the TCF/LEF binding site was mutated. Mutation of the CDX2 binding motif as well as mutation of the overlapping FOX/MYB sites decreased *EPHB2* enhancer activity by 55% and 52%, respectively (Fig. 3D). These results demonstrate that intact binding motifs for CDX2, TCF7L2, FOXA1, and MYB are required for *EPHB2* enhancer functionality and suggest that these transcription factors constitute activators of the *EPHB2* enhancer. Further support for a regulatory function of CDX2, TCF7L2, FOXA1, and MYB at the *EPHB2* gene is provided by a statistically highly significant positive correlation between the expression levels of these factors and that of *EPHB2* in the transcriptomes of colorectal tumors and CRC cell lines (Fig. S5A). However, because of the overlap of the FOXA1 and MYB binding sites, at this point it is not possible to tell whether both or only one of the factors contribute to *EPHB2* enhancer activity.

3.3. Snail1 inactivates the EPHB2 -8.4 kb enhancer by downregulation of its main activators

We next investigated a potential link between the identified enhancer factors and the decommissioning of the *EPHB2* -8.4 kb enhancer through SNAIL1. One possibility was that SNAIL1 targets *CDX2*, *MYB*, and *FOXA1* to indirectly downregulate *EPHB2*. If so, one would expect that their expression parallels that of *EPHB2* in our model of CRC cell lines. In fact, the abundance of the *EPHB2* enhancer factors is reduced or absent in SW480 and HCT116 cells that express endogenous SNAIL1 (Fig. S5B). Likewise, the expression of *CDX2*, *FOXA1*, and *MYB* was significantly decreased upon induction of Snail1-HA in LS174T cells,

16

both on the mRNA and protein level (Fig. 4A,B). The downregulation took place within the first 24 h of Dox treatment and expression levels of *FOXA1* and *MYB* remained well below those of control cells thereafter. In contrast, *CDX2* expression showed full recovery at later time points. To further examine the relationship between *EPHB2* expression and the transcription factors CDX2, FOXA1, MYB, and TCF7L2 as well as the role of SNAIL1 in the regulation of these genes, we performed a pairwise correlation analysis based on the two microarray datasets GSE14333 and GSE59875 described above. The analysis showed that *EPHB2* and its potential activators *CDX2*, *FOXA1*, and *MYB* formed a cluster of genes whose expression was mainly positively correlated among each other (Fig. 4C). Similarly, the EMT-inducers *SNAI1*, *SNAI2*, and *ZEB1* formed a distinct cluster of genes which were positively correlated among each other. Intriguingly, the expression of the genes in the two described clusters was clearly anti-correlated. The described results could be observed in both datasets, in the colorectal tumor samples and in the CRC cell lines, underlining the generality of this observation. The association of *TCF7L2* with either of the two anti-correlated expression clusters was less obvious since its expression only positively correlated with *FOXA1* in both datasets.

We then performed ChIP experiments to investigate the occupancy of CDX2, FOXA1, and MYB at the *EPHB2* -8.4 kb enhancer region *in vivo* and to analyze the effects of the induction of Snail1-HA on the binding of these factors (Fig. 4D). In control cells and in the absence of Snail1-HA, all three transcription factors showed a clear enrichment at the *EPHB2* enhancer region at -8.4 kb compared to a negative control region at -12.3 kb. Furthermore, the induction of Snail1-HA led to a strong decrease in enhancer occupancy for FOXA1 and MYB within 48 h of Dox treatment. However, no significant reduction in CDX2 enrichment was observed upon Snail1-HA expression. From these observations we conclude that the Snail1-HA-induced silencing of *EPHB2* expression involves the downregulation of MYB and FOXA1 and thereby their displacement from the *EPHB2* -8.4 kb enhancer region.

The observed anti-correlation between *EPHB2*, *CDX2*, *FOXA1*, and *MYB* on the one hand, and the EMT inducers *SNAI1*, *SNAI2* and *ZEB1* on the other hand, prompted us to investigate whether other EMT inducers might also be able to repress *EPHB2*. For this we generated LS174T cells that allowed for Dox-inducible expression of ZEB1-HA and SNAIL2-HA. However, neither ZEB1-HA nor SNAIL2-HA expression led to the downregulation of *EPHB2* (Fig. S6). Interestingly, ZEB1-HA and SNAIL2-HA also failed to repress or otherwise deregulate *FOXA1*, *MYB* and *CDX2* (Fig. S6), thereby additionally pointing towards the importance of *MYB* and *FOXA1* downregulation for *EPHB2* enhancer decommissioning.

Thus, SNAIL1 appears to be unique in its ability to repress *EPHB2* expression, most likely because of its distinctive pleiotropic effects.

3.4 Snail1-HA expression induces a TCF7L2/LEF1 switch at the EPHB2 *-8.4 kb enhancer*

EPHB2 is a known Wnt/β-catenin-regulated gene and binding experiments *in vitro* as well as luciferase reporter assays suggested a role for TCF7L2 and the TCF/LEF motif within the *EPHB2* fragment -8398/-8272 for the regulation of *EPHB2* expression. However, in contrast to the expression levels of *CDX2*, *FOXA1*, and *MYB*, no changes in the levels of *TCF7L2* were observed upon the induction of Snail1-HA in LS174T cells (Fig. 5A,B). Interestingly, the expression of *LEF1*, another member of the TCF/LEF family of transcription factors, was strongly up-regulated by Snail1-HA on the mRNA as well as on the protein level (Fig. 5A,B). Notably, the induction of LEF1 expression again was a specific feature of Snail1-HA and could not be observed at comparable levels in LS174T-SNAIL2-HA and LS174T-ZEB1-HA cells (Fig. S6).

To investigate the possible binding of LEF1 to the TCF/LEF motif within the minimal enhancer fragment of *EPHB2*, an *in vitro* binding experiment was performed. Indeed, like TCF7L2, recombinant LEF1 was able to bind to the TCF/LEF motif within the *EPHB2* fragment -8398/-8272 and binding was abolished when the TCF/LEF motif was mutated (Fig. 5C, lanes 3 and 4). Intriguingly, under competitive conditions, the affinity of LEF1 to the TCF/LEF motif was higher than the affinity of TCF7L2 (Fig. 5C, lane 5). This *in vitro* binding result was confirmed by ChIP analyses with living cells (Fig. 5D). Upon the induction of Snail1-HA in LS174T cells the occupancy of TCF7L2 at the *EPHB2* -8.4 kb enhancer region decreased while in parallel an enrichment of LEF1 at the same position was observed. Apparently, upon expression of Snail1-HA, a switch occurs in occupancy of the *EPHB2* 8.4kb enhancer region from TCF7L2 to LEF1.

To determine whether this switch in occupancy might have any consequences for *EPHB2* -8.4 kb enhancer function, we performed luciferase reporter gene assays. Different combinations of expression vectors for TCF7L2, LEF1 and a constitutively active form of β-catenin were cotransfected into LS174T cells together with a reporter plasmid containing the *EPHB2* minimal enhancer fragment. Reporter constructs harboring a mutation in the TCF/LEF binding site of the *EPHB2* minimal enhancer and carrying no *EPHB2* enhancer sequences at all served as controls. Although these experiments revealed a non-specific stimulatory effect of TCF7L2 and LEF1 overexpression on the promoter-only reporter construct, we did not observe functional differences between TCF7L2 and LEF1 in this

18

setting (Fig. S7). In contrast, in the presence of the wild-type *EPHB2* minimal enhancer we found that the combination of β-catenin and TCF7L2 significantly stimulated whereas coexpression of β-catenin and LEF1 reduced *EPHB2* minimal enhancer activity (Fig. S7). As expected, mutation of the TCF/LEF binding motif at the *EPHB2* minimal enhancer decreased reporter gene expression and largely leveled differences between TCF7L2 and LEF1. Especially, the mutation abolished the ability of β-catenin to modulate TCF7L2 and LEF1 activity. This lends support to the specificity of the opposing effects that TCF7L2 and LEF1 had at the wild-type *EPHB2* minimal enhancer in the presence of β-catenin, and argues that LEF1 has a repressive effect on *EPHB2* minimal enhancer activity. Therefore, in addition to the downregulation of FOXA1 and MYB, the TCF7L2/LEF1 switch may also contribute to the decommissioning of the *EPHB2* -8.4 kb enhancer region in the wake of Snail1-HA induction.

3.5 The Lef1-HA/TCF7L2 exchange does not suffice to disrupt the EPHB2 *-8.4 kb enhancer complex and to permanently downregulate* EPHB2

Snail1 appears to disable the *EPHB2* -8.4 kb enhancer by simultaneously displacing or exchanging multiple transcription factors. However, the enhanceosome model for transcriptional enhancers suggests that the dysfunction of a single transcription factor would suffice to completely deactivate an enhancer [42]. Therefore, we were curious to see how a single change in transcription factor composition of the *EPHB2* -8.4 kb enhancer would affect *EPHB2* expression. To this end, we generated LS174T cells that upon Dox treatment express Lef1-HA. Upon induction of Lef1-HA for 24 h, expression of *EPHB2* was significantly downregulated on the mRNA and on the protein level (Fig. 6A,B). Interestingly, at later time points *EPHB2* expression fully recovered. Furthermore, expression analyses for *CDX2*, *FOXA1*, and *MYB* revealed clear differences between cells overexpressing Lef1-HA and Snail1-HA. While Snail1-HA induction had strongly downregulated *FOXA1* and *MYB*, mRNA levels of MYB hardly changed upon expression of Lef1-HA (Fig. 6A) and the observed alterations in MYB protein amounts were not specific for Lef1-HA expressing cells (Fig. 6B). In contrast to what had been observed in Snail1-HA expressing cells, FOXA1 transcript and protein levels actually increased in Lef1-HA expressing cells (Fig. 6A,B). Likewise, Snail1-HA had provoked a temporary but pronounced decrease in *CDX2* expression whereas the transient decrease in *CDX2* transcript quantity was much less extensive in the presence of Lef1-HA (Fig. 6A). The temporary decline in CDX2 protein amounts, however, appeared comparable in Snail1-HA and Lef1-HA expressing cells (compare Figs. 4B and 6B). Moreover, there was no reciprocal induction of *SNAI1* expression in the presence of Lef1-HA.

Next, we wished to determine whether the transient downregulation of *EPHB2* upon expression of Lef1-HA was accompanied by any change in transcription factor occupancy and chromatin structure at the *EPHB2* -8.4 kb enhancer. To gain insight into this aspect, we conducted ChIP and FAIRE analyses. As it had already been seen following the expression of Snail1-HA, a switch between TCF7L2 and Lef1-HA at the *EPHB2* -8.4 kb enhancer was observed (Fig. 6C). Furthermore, at 24 h post-induction of Lef1-HA, levels of the active enhancer mark H3K27ac were decreased in the presence of Lef1-HA (Fig. S8A). This is in agreement with reduced *EPHB2* transcriptional activity at this time point. In contrast, the occupancy of the *EPHB2* -8.4 kb enhancer by FOXA1, MYB, and CDX2 was not altered in Lef1-HA expressing cells (Fig. 6D). We also investigated whether the TCF7L2/Lef1-HA exchange affected the interaction of β-catenin with the *EPHB2* -8.4 kb enhancer. β-Catenin was present at the *EPHB2* -8.4 kb enhancer in control cells and prior to Lef1-HA induction (Fig. S8C). β-Catenin also occupied the enhancer at the 6 h, 24 h and 48 h time points of Lef1-HA expression (Fig. S8C). Likewise, the open chromatin structure at the *EPHB2* -8.4 kb enhancer as indicated by an elevated FAIRE signal and low abundance of H3 remained unchanged despite Lef1-HA occupancy (Fig. S8A,B). Apparently, the Lef1-HA/TCF7L2 exchange does not suffice to disrupt the *EPHB2* -8.4 kb enhancer complex. Nonetheless, these results suggest that the temporary downregulation of *EPHB2* upon Lef1-HA induction might be caused by the switch between TCF7L2 and Lef1-HA. A permanent decrease of *EPHB2* expression, however, seems to be prevented by the continuous occupancy of the *EPHB2* -8.4 kb enhancer by CDX2, FOXA1, MYB and β-catenin.

Finally, we examined whether the expression of *LEF1* and *EPHB2* is negatively correlated similar to what we had seen for *EPHB2* and *SNAI1*. However, there is only a marginal and statistically insignificant anti-correlation between *EPHB2* and *LEF1* expression in the transcriptomes of CRC cell lines and tumors (Fig. S5C). This could be explained by the fact that *LEF1* is not an exclusive target of SNAIL1 and obviously multiple changes in transcription factor expression are needed to inactivate the *EPHB2* -8.4 kb enhancer. Therefore, SNAIL1-independent upregulation of *LEF1* in some CRC cell lines and tumors would not be expected to concur with reduced *EPHB2* levels without the concomitant loss of *MYB* and *FOXA1* expression that we observed to be deregulated by SNAIL1 but not LEF1.

4. Discussion

EPHB2 is an important tumor suppressor gene whose expression is secondarily downregulated during the transition from the non-invasive adenoma to the invasive carcinoma state in a sizable fraction of colorectal cancers [15, 25, 26]. The aim of the present study was to gain insights into the mechanisms that lead to the silencing of *EPHB2* during CRC progression, with a special interest in the roles that the *EPHB2* -8.4 kb enhancer and the EMT-inducer SNAIL1 play in this process. Indeed, Snail1-induced repression of *EPHB2* appears to result from the decommissioning of the *EPHB2* -8.4 kb enhancer. However, Snail1 does not seem to directly act upon this regulatory element. Rather, it inactivates the *EPHB2* -8.4 kb enhancer through the downregulation of FOXA1 and MYB, thereby displacing two activating transcription factors from the enhancer. In addition, Snail1 upregulates LEF1 which in turn replaces TCF7L2 at the *EPHB2* -8.4 kb enhancer region. These changes in transcription factor occupancy are accompanied by a loss of structural hallmarks of active chromatin and lead to the decommissioning of the *EPHB2* -8.4 kb enhancer region and *EPHB2* transcriptional silencing.

4.1. Indirect regulation of EPHB2 by Snail1 and role of the EPHB2 *-8.4 kb enhancer*

There is an anti-correlation between *EPHB2* and *SNAI1* expression in the transcriptomes of CRC cell lines and tumors, and the induction of Snail1 in LS174T cells leads to a massive downregulation of *EPHB2* (this study; [28]). In this regard there is considerable similarity between *EPHB2* and the closely related *EPHB3* gene [28]. However, in contrast to *EPHB3* which is directly repressed by Snail1, we believe that Snail1 inhibits *EPHB2* expression through an indirect mechanism. This is because downregulation of *EPHB2* is delayed compared to the direct Snail1 target genes *EPHB3* and *CDH1* [28]. Moreover, we have not yet been able to demonstrate an interaction of Snail1 with *EPHB2* sequences by EMSA and ChIP (data not shown).

Through bioinformatic and chromatin structural analyses we aimed to identify *cis*-regulatory elements involved in the downregulation of *EPHB2* expression. Previous work from our laboratory had suggested that the *EPHB2* -8.4 kb enhancer could be involved in the differential *EPHB2* expression in a panel of CRC cells but at that time we did not identify relevant transcription factors and therefore the connections between *EPHB2* downregulation, the *EPHB2* -8.4 kb enhancer, and EMT remained unknown [2, 28]. We now show that within -12.3 kb of *EPHB2* upstream sequences, the loss of active chromatin features in *EPHB2*

21

non-expressing cell lines occurs exclusively at the -8.4 kb region. Likewise, induction of Snail1 in LS174T cells causes changes in chromatin accessibility and histone-modifications around the *EPHB2* -8.4 kb enhancer but not at other potential regulatory elements in the 5'-region of *EPHB2*. Therefore, the *EPHB2* -8.4 kb enhancer indeed appears to be intimately connected to Snail1-mediated repression of *EPHB2*.

The results from the chromatin structural analyses were complemented by luciferase reporter experiments. Our mapping studies identified the *EPHB2* DNA sequences from -8398 to -8272 as the smallest fragment that has enhancer activity in luciferase assays with CRC cell lines. Importantly, the *EPHB2* minimal enhancer fragment exhibits cell-type-specificity that exactly parallels expression of the endogenous *EPHB2* gene. This further supports the idea that the *EPHB2* enhancer plays a key role in controlling *EPHB2* expression and that inactivation of the enhancer underlies *EPHB2* silencing.

The *EPHB2* minimal enhancer fragment is located within one of the ECRs in the *EPHB2* upstream region. Interestingly, the position of this ECR and the *EPHB2* minimal enhancer fragment do not exactly match a region that shows DNaseI hypersensitivity and high levels of H3K4me1 and H3K27ac. This apparent discrepancy could be explained by the observation that enhancer core regions are usually devoid of histones. Therefore, histone modifications can be identified only in regions flanking enhancer cores [43]. It should also be kept in mind that the ENCODE data for DNaseI hypersensitivity and the enrichment of H3K4me1 and H3K27ac at the *EPHB2* locus were derived from HUVEC cells. There are three ECRs between -9.0 kb and -7.5 kb upstream of the *EPHB2* TSS. It is possible that these ECRs represent a cluster of regulatory elements that either individually or in combination control *EPHB2* expression in different tissues. Accordingly, the *EPHB2* -8.4 kb region could represent an intestine-specific regulatory element whereas *EPHB2* expression in HUVEC cells might be driven by an adjacent, more promoter-proximal element.

4.2. Transcription factors required for EPHB2 enhancer function

In silico analyses identified a cluster of transcription factor binding sites within the *EPHB2* minimal enhancer fragment. By EMSA and ChIP we confirmed that CDX2, FOXA1, MYB, and TCF7L2 bind to the *EPHB2* minimal enhancer region *in vitro* and in *EPHB2* expressing cells. Our findings agree with the results of earlier studies that demonstrated the occupancy of the *EPHB2* enhancer region by TCF7L2 and CDX2 [2, 44, 45] but the interaction of FOXA1 and MYB with this element was not previously known. In functional assays, mutation

of the CDX2, FOX/MYB, and TCF/LEF binding motifs led to a loss of enhancer activity. These novel findings provide strong evidence that CDX2, FOXA1, MYB, and TCF7L2 are important components of the *EPHB2* enhancer transcription factor complex and function as transcriptional activators of the *EPHB2* gene. However, we cannot rule out that additional transcription factors are involved in the regulation and maintenance of *EPHB2* enhancer function because our analyses concentrated on the *EPHB2* minimal enhancer. This was motivated by the cell-type-specific activity pattern of this element which reflects the expression of the endogenous *EPHB2* gene. Nonetheless, as DNA sequence conservation and regions characterized by DNaseI hypersensitivity and H3K4me1/H3K27ac enrichment extend beyond the *EPHB2* minimal enhancer, further transcription factors may contribute to the activity of the native *EPHB2* enhancer in its chromosomal context.

In our DNA binding experiments *in vitro* we observed that CDX2 formed two distinct protein::DNA complexes although only a single CDX2 consensus binding motif within the *EPHB2* minimal enhancer had been predicted. Both CDX2::DNA complexes completely disappeared when the single predicted CDX2 binding site was mutated. This implies that formation of the more slowly migrating CDX2::DNA complex critically depends upon CDX2 self-interactions. In support of this idea, it was previously demonstrated that CDX2 has the capability of forming dimers [46]. Because CDX2 dimerization appears to be aided by the presence of variably spaced palindromic binding motifs [46], it cannot be ruled out that formation of CDX2 dimers at the *EPHB2* minimal enhancer is supported to some extent through additional DNA contacts of CDX2 with cryptic binding sites.

Similar to CDX2, FOXA1 also generated two DNA complexes in EMSA analyses. In contrast to CDX2, however, formation of multiple FOXA1::DNA complexes probably is not due to dimerization [47, 48] but instead results from the presence of multiple FOXA1 binding motifs within the *EPHB2* minimal enhancer fragment. In agreement with this idea, only one of the two FOXA1::DNA complexes completely disappeared while the other one was diminished when the mutated probe was used. Binding sites for members of the family of Forkhead domain DNA binding proteins are known to exhibit a fairly high degree of degeneracy [47], which could explain the difficulty of reliably detecting FOXA1 binding motifs by *in silico* analysis.

Curiously, the FOXA1 binding site that we identified and that was confirmed by EMSA and mutagenesis overlaps with a validated binding motif for the MYB transcription factor. In addition, ChIP analyses demonstrated occupancy of the *EPHB2* enhancer by both factors in LS174T cells. This raises the question of how FOXA1 and MYB function at the *EPHB2*

23

enhancer. One possibility is that there are different cell populations in which FOXA1 and MYB alternatively occupy the *EPHB2* enhancer. On the other hand, FOXA1 and MYB might simultaneously interact with the *EPHB2* enhancer by virtue of distinct modes of DNA recognition [48, 49]. The co-occurrence of FOXA1 and MYB motifs and the cooperation between FOXA1 and MYB in chromatin binding at enhancer regions was previously described [50] and the overlapping FOXA1/MYB motifs at the *EPHB2* enhancer could provide an example for the recently described phenomenon of unconventional composite DNA binding sites that form the basis for heterotypic transcription factor cooperations [51].

CDX2, FOXA1, MYB, and TCF7L2 are transcription factors with well described functions in intestinal development and tissue homeostasis. CDX2 is a homeobox transcription factor with important roles in anterior-posterior patterning of the gastro-intestinal tract as well as control of gene expression along the crypt-villus axis [40, 52-54]. FOX proteins, including FOXA1, are involved in the specification and patterning of endoderm and its derivatives, and a contribution of FOXA1 to the differentiation of enteroendocrine and goblet cells has previously been shown [41, 55]. *MYB* is a proto-oncogene that was shown to control the self-renewal capacity of intestinal stem cells, most likely by regulating the expression of critical stem cell genes such as *LGR5* [37]. Of note, like *LGR5*, *EPHB2* is part of the intestinal stem cell signature [56]. TCF7L2 belongs to the TCF/LEF family of transcription factors which are well described mediators of the Wnt/β-catenin signaling pathway. Wnt/β-catenin signaling and TCF7L2 are required for the maintenance of the intestinal stem cell compartment [38] and *EPHB2* was reported to be a Wnt/β-catenin target gene [12]. Altogether, in view of their known roles in the development and tissue homeostasis of the intestinal epithelium it is quite plausible that CDX2, FOXA1, MYB, and TCF7L2 converge on the *EPHB2* -8.4 kb enhancer to collectively control *EPHB2* expression.

4.3. Enhancer inactivation through Snail1

How does Snail1 incapacitate the *EPHB2* -8.4 kb enhancer? Our results suggest that the induction of Snail1 in LS174T cells triggers multiple changes in gene expression and transcription factor occupancy that culminate in the decommissioning of the *EPHB2* -8.4 kb enhancer (Fig. 6E). For one, *FOXA1* and *MYB* are downregulated in the presence of Snail1. This leads to a strong reduction of FOXA1 and MYB occupancy at the *EPHB2* -8.4 kb enhancer which thereby is deprived of two of its activators. Moreover, LEF1 is upregulated by Snail1 and competitively displaces TCF7L2 from the *EPHB2* -8.4 kb enhancer. LEF1 has a higher affinity for TCF/LEF binding sites compared to TCF7L2, not only at the *EPHB2* -8.4

kb enhancer but also at other target genes [34, 57]. This is likely to facilitate the TCF7L2/LEF1 exchange once LEF1 levels rise. It is conceivable that the replacement of TCF7L2 by LEF1 affects *EPHB2* -8.4 kb enhancer function since TCF7L2 and LEF1 are functionally distinct [34, 58, 59], and LEF1 overexpression had a repressive effect on *EPHB2* minimal enhancer activity in luciferase reporter assays. Intriguingly, repressor functions of LEF1 in colorectal cancer cells [60] and at the *CDH1* gene are known [61]. Hence, the exchange of two functionally distinct TCF/LEF family members may very well disconnect the *EPHB2* -8.4 kb enhancer from the Wnt/β-catenin pathway. The continuous occupancy of the *EPHB2* -8.4 kb enhancer by β-catenin despite the TCF7L2/LEF1 exchange is not necessarily in conflict with this view because there are precedents for the presence of β-catenin at genes that are negatively regulated by Wnt/β-catenin signaling [61, 62]. Ultimately, the combined loss of several activators probably in conjunction with some of their associated co-factors in turn might cause the observed reduction in H3K27ac levels and an increase in H3 occupancy.

In contrast to *FOXA1* and *MYB*, the expression of *CDX2* is only transiently downregulated by Snail1, and CDX2 appears to remain associated with the *EPHB2* -8.4 kb enhancer upon Snail1 induction. The continuous occupancy by CDX2 could be the reason for the incomplete collapse of *EPHB2* -8.4 kb enhancer chromatin upon Snail1 induction which we observed in our FAIRE analyses. The additional loss of *CDX2* expression as seen in HCT116 and SW480 [63] cells might explain the more complete chromatin compaction at the *EPHB2* -8.4 kb enhancer in these cells.

The model for *EPHB2* transcriptional silencing and the pathophysiological relevance of the regulatory relationships among *SNAIL1*, *LEF1*, *CDX2*, *FOXA1*, *MYB*, and *EPHB2* are supported by several additional observations. In contrast to Snail1, two other well-characterized EMT transcription factors SNAIL2 and ZEB1 did not repress *EPHB2*. Intriguingly, SNAIL2 and ZEB1 also failed to downregulate *FOXA1*, *MYB* and *CDX2* and only weakly stimulated *LEF1* expression. These findings are in agreement with the proposed model for *EPHB2* repression that postulates the necessity for multiple concurrent changes in transcription factor expression and *EPHB2* -8.4 kb enhancer occupancy. Furthermore, transcriptome analysis revealed an anti-correlated expression of *SNAIL1* on the one hand, and of *CDX2*, *MYB*, *FOXA1,* and *EPHB2* on the other hand in a broad range of CRC cell lines and a large number of tumors. In agreement with upregulation of *LEF1* in LS174T cells downstream of Snail1, it has been observed that *LEF1* is also induced during EMT in other model systems [64-66]. This regulation of LEF1 appears to occur indirectly and likely involves a cascade of gene expression changes which ultimately trigger LEF1 induction

25

through the activation of SMAD proteins [65]. SMADs can be activated by TGFβ and BMP signaling pathways both of which are known to positively regulate *LEF1* [65, 67]. Importantly, LS174T cells are SMAD4-positive, have a functional BMP pathway [68] and *BMP2* and *BMP4* are upregulated in the presence of Snail1-HA (Fig. S9). Taken together, these observations provide strong evidence that Snail1-HA indirectly induces LEF1 expression through a BMP/SMAD axis. Furthermore, with respect to the other transcription factors involved in the regulation of *EPHB2* expression and their role in tumor progression and EMT, it was shown that RNAi-mediated silencing of *FOXA1* and *FOXA2* is sufficient to induce EMT by downregulation of epithelial markers, such as *CDH1*, and it was argued that *FOXA1* exerts a so called roadblock function in EMT [69]. Like *EPHB2*, *CDX2* functions as tumor suppressor in CRC and *CDX2* expression is frequently lost during tumor progression. The role of MYB, however, is somewhat ambiguous. MYB was reported to promote EMT in different human cancer cells by the upregulation of *SNAI2* [70], but *MYB* itself is rapidly downregulated in a breast cancer model of Snail1-induced EMT and *MYB* appears to be a direct target of ZEB1 in this context [71, 72]. Furthermore, several studies demonstrate a better prognosis and reduced metastasis in breast cancers with high expression of *MYB* [73]. Downregulation by EMT inducers and potential anti-metastatic activity would be consistent with the proposed role of MYB as an activator of a tumor and invasion suppressor gene such as *EPHB2*.

When compared to Snail1, overexpression of Lef1 and replacement of TCF7L2 by Lef1 at the *EPHB2* -8.4 kb enhancer without concomitant downregulation of *FOXA1* and *MYB* only had a mild effect on *EPHB2* expression and did not suffice to repress *EPHB2* for an extended period of time. The drop in *EPHB2* expression was reflected by a decrease in the levels of H3K27ac, a chromatin mark that specifies active enhancers. Aside from that, *EPHB2* -8.4 kb enhancer chromatin remained in an open conformation and CDX2, FOXA1, MYB, and β-catenin continued to occupy the *EPHB2* -8.4 kb enhancer. Overall, these findings are in conflict with the enhanceosome model for enhancer function that proposes a high degree of cooperation between different enhancer-bound transcription factors. Accordingly, the lack of just one of these factors should be sufficient to impair enhancer function by disrupting the enhanceosome [42]. However, mutational analyses of the *EPHB2* -8.4 kb enhancer by luciferase reporter assays showed that the mutation of single transcription factor binding sites did not completely abolish enhancer activity. This result also argues that transcription factors can associate with the *EPHB2* -8.4 kb enhancer largely independently from each other and thereby support partial enhancer function. Likewise, CDX2 remained at the *EPHB2* -8.4 kb enhancer even upon dissociation of FOXA1, MYB, and TCF7L2. It seems as though the *EPHB2* -8.4 kb enhancer adheres to the billboard

model for enhancer function. This model describes each enhancer factor or small group of factors as an independently acting unit and postulates that the loss of one of these units has only minor effects on the overall enhancer function [74]. Irrespective of which type of model applies to the *EPHB2* -8.4 kb enhancer, it is nonetheless conceivable that the removal of only one component is not sufficient to dismantle huge, multi-component protein complexes that are formed by transcription factors together with their co-activators. In support of this view, it was recently described that EMT-associated repression of *CDH1* also requires multiple assaults including the direct binding of Snail1 to the *CDH1* promoter and the inactivation of two transcriptional enhancers by downregulation of Grhl3 and Hnf4α [75]. Similarly, inactivation of the *EPHB3* enhancer is a multimodal process that involves the repression and competitive displacement of transcriptional activators by Snail1 [28].

Enhancers are of utmost importance for the spatiotemporal orchestration of gene expression patterns for instance in development, adult life, cellular reprogramming, or tumorigenesis. Much work is dedicated to the understanding of enhancer activation during development and to mechanisms of enhancer action. In contrast, surprisingly little is known about the inactivation of enhancers although this process contributes essentially to the reshaping of gene expression programs. In fact, during tumor progression, the loss of active enhancers prevails over the gain of functional enhancers [76-78], and many fibroblast-specific enhancers are decommissioned in the earliest phases of reprogramming [79]. The deregulation of multiple factors and combinatorial attacks on enhancer and/or promoter transcriptional complexes could be a more common mechanism to effectively silence gene expression.

References

[1] T.K. Kim, R. Shiekhattar, Architectural and Functional Commonalities between Enhancers and Promoters, Cell, 162 (2015) 948-959.

[2] S. Jägle, K. Rönsch, S. Timme, H. Andrlová, M. Bertrand, M. Jäger, A. Proske, M. Schrempp, A. Yousaf, T. Michoel, R. Zeiser, M. Werner, S. Lassmann, A. Hecht, Silencing of the EPHB3 tumor-suppressor gene in human colorectal cancer through decommissioning of a transcriptional enhancer, Proc Natl Acad Sci USA, 111 (2014) 4886-4891.

[3] L. Pasquali, K.J. Gaulton, S.A. Rodriguez-Segui, L. Mularoni, I. Miguel-Escalada, I. Akerman, J.J. Tena, I. Moran, C. Gomez-Marin, M. van de Bunt, J. Ponsa-Cobas, N. Castro, T. Nammo, I. Cebola, J. Garcia-Hurtado, M.A. Maestro, F. Pattou, L. Piemonti, T. Berney, A.L. Gloyn, P. Ravassard, J.L. Gomez-Skarmeta, F. Muller, M.I. McCarthy, J. Ferrer, Pancreatic islet enhancer clusters enriched in type 2 diabetes risk-associated variants, Nat Genetics, 46 (2014) 136-143.

[4] M.R. Mansour, B.J. Abraham, L. Anders, A. Berezovskaya, A. Gutierrez, A.D. Durbin, J. Etchin, L. Lawton, S.E. Sallan, L.B. Silverman, M.L. Loh, S.P. Hunger, T. Sanda, R.A. Young, A.T. Look, Oncogene regulation. An oncogenic super-enhancer formed through somatic mutation of a noncoding intergenic element, Science, 346 (2014) 1373-1377.

[5] R.C. Poulos, M.A. Sloane, L.B. Hesson, J.W. Wong, The search for cis-regulatory driver mutations in cancer genomes, Oncotarget, 6 (2015) 32509-32525.

[6] R. Kalluri, R.A. Weinberg, The basics of epithelial-mesenchymal transition, J Clin Inv, 119 (2009) 1420-1428.

[7] S. Lamouille, J. Xu, R. Derynck, Molecular mechanisms of epithelial-mesenchymal transition, Nat Rev Mol Cell Biol, 15 (2014) 178-196.

[8] K.R. Fischer, A. Durrans, S. Lee, J. Sheng, F. Li, S.T. Wong, H. Choi, T. El Rayes, S. Ryu, J. Troeger, R.F. Schwabe, L.T. Vahdat, N.K. Altorki, V. Mittal, D. Gao, Epithelial-to-mesenchymal transition is not required for lung metastasis but contributes to chemoresistance, Nature, 527 (2015) 472-476.

[9] W.L. Hwang, J.K. Jiang, S.H. Yang, T.S. Huang, H.Y. Lan, H.W. Teng, C.Y. Yang, Y.P. Tsai, C.H. Lin, H.W. Wang, M.H. Yang, MicroRNA-146a directs the symmetric division of Snail-dominant colorectal cancer stem cells, Nat Cell Biol, 16 (2014) 268-280.

[10] P. Zhang, Y. Wei, L. Wang, B.G. Debeb, Y. Yuan, J. Zhang, J. Yuan, M. Wang, D. Chen, Y. Sun, W.A. Woodward, Y. Liu, D.C. Dean, H. Liang, Y. Hu, K.K. Ang, M.C. Hung, J. Chen, L. Ma, ATM-mediated stabilization of ZEB1 promotes DNA damage response and radioresistance through CHK1, Nat Cell Biol, 16 (2014) 864-875.

[11] X. Zheng, J.L. Carstens, J. Kim, M. Scheible, J. Kaye, H. Sugimoto, C.C. Wu, V.S. LeBleu, R. Kalluri, Epithelial-to-mesenchymal transition is dispensable for metastasis but induces chemoresistance in pancreatic cancer, Nature, 527 (2015) 525-530.

[12] E. Batlle, J.T. Henderson, H. Beghtel, M.M. van den Born, E. Sancho, G. Huls, J. Meeldijk, J. Robertson, M. van de Wetering, T. Pawson, H. Clevers, Beta-catenin and TCF mediate cell positioning in the intestinal epithelium by controlling the expression of EphB/ephrinB, Cell, 111 (2002) 251-263.

[13] A. Merlos-Suarez, E. Batlle, Eph-ephrin signalling in adult tissues and cancer, Curr Opin Cell Biol, 20 (2008) 194-200.

[14] M. Genander, M.M. Halford, N.J. Xu, M. Eriksson, Z. Yu, Z. Qiu, A. Martling, G. Greicius, S. Thakar, T. Catchpole, M.J. Chumley, S. Zdunek, C. Wang, T. Holm, S.P. Goff, S. Pettersson, R.G. Pestell, M. Henkemeyer, J. Frisen, Dissociation of EphB2 signaling pathways mediating progenitor cell proliferation and tumor suppression, Cell, 139 (2009) 679-692.

[15] E. Batlle, J. Bacani, H. Begthel, S. Jonkheer, A. Gregorieff, M. van de Born, N. Malats, E. Sancho, E. Boon, T. Pawson, S. Gallinger, S. Pals, H. Clevers, EphB receptor activity suppresses colorectal cancer progression, Nature, 435 (2005) 1126-1130.

[16] C. Cortina, S. Palomo-Ponce, M. Iglesias, J.L. Fernandez-Masip, A. Vivancos, G. Whissell, M. Huma, N. Peiro, L. Gallego, S. Jonkheer, A. Davy, J. Lloreta, E. Sancho, E. Batlle, EphB-ephrin-B interactions suppress colorectal cancer progression by compartmentalizing tumor cells, Nat Genetics, 39 (2007) 1376-1383.

[17] M. van de Wetering, E. Sancho, C. Verweij, W. de Lau, I. Oving, A. Hurlstone, K. van der Horn, E. Batlle, D. Coudreuse, A.P. Haramis, M. Tjon-Pon-Fong, P. Moerer, M. van den Born, G. Soete, S. Pals, M. Eilers, R. Medema, H. Clevers, The beta-catenin/TCF-4 complex imposes a crypt progenitor phenotype on colorectal cancer cells, Cell, 111 (2002) 241-250.

[18] L.G. van der Flier, H. Clevers, Stem cells, self-renewal, and differentiation in the intestinal epithelium, Ann Rev Physiol, 71 (2009) 241-260.

[19] L.E. Dow, K.P. O'Rourke, J. Simon, D.F. Tschaharganeh, J.H. van Es, H. Clevers, S.W. Lowe, Apc Restoration Promotes Cellular Differentiation and Reestablishes Crypt Homeostasis in Colorectal Cancer, Cell, 161 (2015) 1539-1552.

[20] K.M. Cadigan, M.L. Waterman, TCF/LEFs and Wnt signaling in the nucleus, Cold Spring Harbor perspectives in biology, 4 (2012).

[21] F.A. Atcha, A. Syed, B. Wu, N.P. Hoverter, N.N. Yokoyama, J.H. Ting, J.E. Munguia, H.J. Mangalam, J.L. Marsh, M.L. Waterman, A unique DNA binding domain converts T-cell factors into strong Wnt effectors, Mol Cell Biol, 27 (2007) 8352-8363.

[22] N.P. Hoverter, M.D. Zeller, M.M. McQuade, A. Garibaldi, A. Busch, E.M. Selwan, K.J. Hertel, P. Baldi, M.L. Waterman, The TCF C-clamp DNA binding domain expands the Wnt transcriptome via alternative target recognition, Nucl Acids Res, 42 (2014) 13615-13632.

[23] B. Wallmen, M. Schrempp, A. Hecht, Intrinsic properties of Tcf1 and Tcf4 splice variants determine cell-type-specific Wnt/beta-catenin target gene expression, Nucl Acids Res, 40 (2012) 9455-9469.

[24] A. Weise, K. Bruser, S. Elfert, B. Wallmen, Y. Wittel, S. Wohrle, A. Hecht, Alternative splicing of Tcf7l2 transcripts generates protein variants with differential promoter-binding and transcriptional activation properties at Wnt/beta-catenin targets, Nucl Acids Res, 38 (2010) 1964-1981.

[25] K. Rönsch, M. Jäger, A. Schopflin, M. Danciu, S. Lassmann, A. Hecht, Class I and III HDACs and loss of active chromatin features contribute to epigenetic silencing of CDX1 and EPHB tumor suppressor genes in colorectal cancer, Epigenetics, 6 (2011) 610-622.

[26] D.L. Guo, J. Zhang, S.T. Yuen, W.Y. Tsui, A.S. Chan, C. Ho, J. Ji, S.Y. Leung, X. Chen, Reduced expression of EphB2 that parallels invasion and metastasis in colorectal tumours, Carcinogenesis, 27 (2006) 454-464.

[27] A. Lugli, H. Spichtin, R. Maurer, M. Mirlacher, J. Kiefer, P. Huusko, D. Azorsa, L. Terracciano, G. Sauter, O.P. Kallioniemi, S. Mousses, L. Tornillo, EphB2 expression across 138 human tumor types in a tissue microarray: high levels of expression in gastrointestinal cancers, Clin Cancer Res, 11 (2005) 6450-6458.

[28] K. Rönsch, S. Jägle, K. Rose, M. Seidl, F. Baumgartner, V. Freihen, A. Yousaf, E. Metzger, S. Lassmann, R. Schüle, R. Zeiser, T. Michoel, A. Hecht, SNAIL1 combines competitive displacement of ASCL2 and epigenetic mechanisms to rapidly silence the EPHB3 tumor suppressor in colorectal cancer, Molecular oncology, 9 (2015) 335-354.

[29] I. Ovcharenko, M.A. Nobrega, G.G. Loots, L. Stubbs, ECR Browser: a tool for visualizing and accessing data from comparisons of multiple vertebrate genomes, Nucl Acids Res, 32 (2004) W280-286.

[30] X. Xie, P. Rigor, P. Baldi, MotifMap: a human genome-wide map of candidate regulatory motif sites, Bioinformatics, 25 (2009) 167-174.

[31] A. Mathelier, X. Zhao, A.W. Zhang, F. Parcy, R. Worsley-Hunt, D.J. Arenillas, S. Buchman, C.Y. Chen, A. Chou, H. Ienasescu, J. Lim, C. Shyr, G. Tan, M. Zhou, B. Lenhard, A. Sandelin, W.W. Wasserman, JASPAR 2014: an extensively expanded and updated open-access database of transcription factor binding profiles, Nucl Acids Res, 42 (2014) D142-147.

[32] W.J. Kent, C.W. Sugnet, T.S. Furey, K.M. Roskin, T.H. Pringle, A.M. Zahler, D. Haussler, The human genome browser at UCSC, Genome Res, 12 (2002) 996-1006.

[33] D.L. Turner, H. Weintraub, Expression of achaete-scute homolog 3 in Xenopus embryos converts ectodermal cells to a neural fate, Genes Dev, 8 (1994) 1434-1447.

[34] A. Hecht, M.P. Stemmler, Identification of a promoter-specific transcriptional activation domain at the C terminus of the Wnt effector protein T-cell factor 4, J Biol Chem, 278 (2003) 3776-3785.

[35] B.T. Preca, K. Bajdak, K. Mock, V. Sundararajan, J. Pfannstiel, J. Maurer, U. Wellner, U.T. Hopt, T. Brummer, S. Brabletz, T. Brabletz, M.P. Stemmler, A self-enforcing CD44s/ZEB1 feedback loop maintains EMT and stemness properties in cancer cells, Int J Cancer, 137 (2015) 2566-2577.

[36] A. Welman, J. Barraclough, C. Dive, Generation of cells expressing improved doxycycline-regulated reverse transcriptional transactivator rtTA2S-M2, Nat Protocols, 1 (2006) 803-811.

[37] D. Cheasley, L. Pereira, S. Lightowler, E. Vincan, J. Malaterre, R.G. Ramsay, Myb controls intestinal stem cell genes and self-renewal, Stem cells, 29 (2011) 2042-2050.

[38] V. Korinek, N. Barker, P. Moerer, E. van Donselaar, G. Huls, P.J. Peters, H. Clevers, Depletion of epithelial stem-cell compartments in the small intestine of mice lacking Tcf-4, Nat Genetics, 19 (1998) 379-383.

[39] J. Malaterre, M. Carpinelli, M. Ernst, W. Alexander, M. Cooke, S. Sutton, S. Dworkin, J.K. Heath, J. Frampton, G. McArthur, H. Clevers, D. Hilton, T. Mantamadiotis, R.G. Ramsay, c-Myb is required for progenitor cell homeostasis in colonic crypts, Proc Natl Acad Sci USA, 104 (2007) 3829-3834.

[40] A.K. San Roman, A. Tovaglieri, D.T. Breault, R.A. Shivdasani, Distinct Processes and Transcriptional Targets Underlie CDX2 Requirements in Intestinal Stem Cells and Differentiated Villus Cells, Stem Cell Rep, 5 (2015) 673-681.

[41] D.Z. Ye, K.H. Kaestner, Foxa1 and Foxa2 control the differentiation of goblet and enteroendocrine L- and D-cells in mice, Gastroenterology, 137 (2009) 2052-2062.

[42] M. Merika, D. Thanos, Enhanceosomes, Curr Opin Genet Dev, 11 (2001) 205-208.

[43] Y. Nie, H. Liu, X. Sun, The patterns of histone modifications in the vicinity of transcription factor binding sites in human lymphoblastoid cell lines, PLOS ONE, 8 (2013) e60002.

[44] P. Hatzis, L.G. van der Flier, M.A. van Driel, V. Guryev, F. Nielsen, S. Denissov, I.J. Nijman, J. Koster, E.E. Santo, W. Welboren, R. Versteeg, E. Cuppen, M. van de Wetering, H. Clevers, H.G. Stunnenberg, Genome-wide pattern of TCF7L2/TCF4 chromatin occupancy in colorectal cancer cells, Mol Cell Biol, 28 (2008) 2732-2744.

[45] M.P. Verzi, P. Hatzis, R. Sulahian, J. Philips, J. Schuijers, H. Shin, E. Freed, J.P. Lynch, D.T. Dang, M. Brown, H. Clevers, X.S. Liu, R.A. Shivdasani, TCF4 and CDX2, major transcription factors for intestinal function, converge on the same cis-regulatory regions, Proc Natl Acad Sci USA, 107 (2010) 15157-15162.

[46] E. Suh, L. Chen, J. Taylor, P.G. Traber, A homeodomain protein related to caudal regulates intestine-specific gene transcription, Mol Cell Biol, 14 (1994) 7340-7351.

[47] B.A. Benayoun, S. Caburet, R.A. Veitia, Forkhead transcription factors: key players in health and disease, Trends Genet, 27 (2011) 224-232.

[48] L.A. Cirillo, K.S. Zaret, Specific interactions of the wing domains of FOXA1 transcription factor with DNA, J Mol Biol, 366 (2007) 720-724.

[49] K. Ogata, S. Morikawa, H. Nakamura, A. Sekikawa, T. Inoue, H. Kanai, A. Sarai, S. Ishii, Y. Nishimura, Solution structure of a specific DNA complex of the Myb DNA-binding domain with cooperative recognition helices, Cell, 79 (1994) 639-648.

[50] C. Zhang, L. Wang, D. Wu, H. Chen, Z. Chen, J.M. Thomas-Ahner, D.L. Zynger, J. Eeckhoute, J. Yu, J. Luo, M. Brown, S.K. Clinton, K.P. Nephew, T.H. Huang, W. Li, Q. Wang, Definition of a FoxA1 Cistrome that is crucial for G1 to S-phase cell-cycle transit in castration-resistant prostate cancer, Cancer Res, 71 (2011) 6738-6748.

[51] A. Jolma, Y. Yin, K.R. Nitta, K. Dave, A. Popov, M. Taipale, M. Enge, T. Kivioja, E. Morgunova, J. Taipale, DNA-dependent formation of transcription factor pairs alters their binding specificity, Nature, 527 (2015) 384-388.

[52] R.J. Guo, E.R. Suh, J.P. Lynch, The role of Cdx proteins in intestinal development and cancer, Cancer Biol Therapy, 3 (2004) 593-601.

[53] A. Hryniuk, S. Grainger, J.G. Savory, D. Lohnes, Cdx function is required for maintenance of intestinal identity in the adult, Dev Biol, 363 (2012) 426-437.

[54] M.P. Verzi, H. Shin, L.L. Ho, X.S. Liu, R.A. Shivdasani, Essential and redundant functions of caudal family proteins in activating adult intestinal genes, Mol Cell Biol, 31 (2011) 2026-2039.

[55] A.M. Zorn, J.M. Wells, Vertebrate endoderm development and organ formation, Ann Rev Dev Biol, 25 (2009) 221-251.

[56] J. Munoz, D.E. Stange, A.G. Schepers, M. van de Wetering, B.K. Koo, S. Itzkovitz, R. Volckmann, K.S. Kung, J. Koster, S. Radulescu, K. Myant, R. Versteeg, O.J. Sansom, J.H. van Es, N. Barker, A. van Oudenaarden, S. Mohammed, A.J. Heck, H. Clevers, The Lgr5 intestinal stem cell signature: robust expression of proposed quiescent '+4' cell markers, EMBO J, 31 (2012) 3079-3091.

[57] T. Pukrop, D. Gradl, K.A. Henningfeld, W. Knochel, D. Wedlich, M. Kuhl, Identification of two regulatory elements within the high mobility group box transcription factor XTCF-4, J Biol Chem, 276 (2001) 8968-8978.

[58] N.P. Hoverter, J.H. Ting, S. Sundaresh, P. Baldi, M.L. Waterman, A WNT/p21 circuit directed by the C-clamp, a sequence-specific DNA binding domain in TCFs, Mol Cell Biol, 32 (2012) 3648-3662.

[59] S. Wöhrle, B. Wallmen, A. Hecht, Differential control of Wnt target genes involves epigenetic mechanisms and selective promoter occupancy by T-cell factors, Mol Cell Biol, 27 (2007) 8164-8177.

[60] K. Rai, S. Sarkar, T.J. Broadbent, M. Voas, K.F. Grossmann, L.D. Nadauld, S. Dehghanizadeh, F.T. Hagos, Y. Li, R.K. Toth, S. Chidester, T.M. Bahr, W.E. Johnson, B. Sklow, R. Burt, B.R. Cairns, D.A. Jones, DNA demethylase activity maintains intestinal cells in an undifferentiated state following loss of APC, Cell, 142 (2010) 930-942.

[61] C. Jamora, R. DasGupta, P. Kocieniewski, E. Fuchs, Links between signal transduction, transcription and adhesion in epithelial bud development, Nature, 422 (2003) 317-322.

[62] T.A. Blauwkamp, M.V. Chang, K.M. Cadigan, Novel TCF-binding sites specify transcriptional repression by Wnt signalling, EMBO J, 27 (2008) 1436-1446.

[63] T. Hinoi, M. Loda, E.R. Fearon, Silencing of CDX2 expression in colon cancer via a dominant repression pathway, J Biol Chem, 278 (2003) 44608-44616.

[64] S. Guaita, I. Puig, C. Franci, M. Garrido, D. Dominguez, E. Batlle, E. Sancho, S. Dedhar, A.G. De Herreros, J. Baulida, Snail induction of epithelial to mesenchymal transition in tumor cells is accompanied by MUC1 repression and ZEB1 expression, J Biol Chem, 277 (2002) 39209-39216.

[65] D. Medici, E.D. Hay, B.R. Olsen, Snail and Slug promote epithelial-mesenchymal transition through beta-catenin-T-cell factor-4-dependent expression of transforming growth factor-beta3, Mol Biol Cell, 19 (2008) 4875-4887.

[66] G. Solanas, M. Porta-de-la-Riva, C. Agusti, D. Casagolda, F. Sanchez-Aguilera, M.J. Larriba, F. Pons, S. Peiro, M. Escriva, A. Munoz, M. Dunach, A.G. de Herreros, J. Baulida, E-cadherin controls beta-catenin and NF-kappaB transcriptional activity in mesenchymal gene expression, J Cell Sci, 121 (2008) 2224-2234.

[67] K. Kratochwil, M. Dull, I. Farinas, J. Galceran, R. Grosschedl, Lef1 expression is activated by BMP-4 and regulates inductive tissue interactions in tooth and hair development, Genes Dev, 10 (1996) 1382-1394.

[68] A. Lorente-Trigos, F. Varnat, A. Melotti, A. Ruiz i Altaba, BMP signaling promotes the growth of primary human colon carcinomas in vivo, J Mol Cell Biol, 2 (2010) 318-332.

[69] Y. Song, M.K. Washington, H.C. Crawford, Loss of FOXA1/2 is essential for the epithelial-to-mesenchymal transition in pancreatic cancer, Cancer Res, 70 (2010) 2115-2125.

[70] B. Tanno, F. Sesti, V. Cesi, G. Bossi, G. Ferrari-Amorotti, R. Bussolari, D. Tirindelli, B. Calabretta, G. Raschella, Expression of Slug is regulated by c-Myb and is required for invasion and bone marrow homing of cancer cells of different origin, J Biol Chem, 285 (2010) 29434-29445.

[71] H.J. Hugo, L. Pereira, R. Suryadinata, Y. Drabsch, T.J. Gonda, N.P. Gunasinghe, C. Pinto, E.T. Soo, B.J. van Denderen, P. Hill, R.G. Ramsay, B. Sarcevic, D.F. Newgreen, E.W. Thompson, Direct repression of MYB by ZEB1 suppresses proliferation and epithelial gene expression during epithelial-to-mesenchymal transition of breast cancer cells, Breast Cancer Res, 15 (2013) R113.

[72] S. Javaid, J. Zhang, E. Anderssen, J.C. Black, B.S. Wittner, K. Tajima, D.T. Ting, G.A. Smolen, M. Zubrowski, R. Desai, S. Maheswaran, S. Ramaswamy, J.R. Whetstine, D.A. Haber, Dynamic chromatin modification sustains epithelial-mesenchymal transition following inducible expression of Snail-1, Cell Rep, 5 (2013) 1679-1689.

[73] M. Nicolau, A.J. Levine, G. Carlsson, Topology based data analysis identifies a subgroup of breast cancers with a unique mutational profile and excellent survival, Proc Natl Acad Sci USA, 108 (2011) 7265-7270.

[74] M.M. Kulkarni, D.N. Arnosti, Information display by transcriptional enhancers, Development, 130 (2003) 6569-6575.

[75] H. Alotaibi, M.F. Basilicata, H. Shehwana, T. Kosowan, I. Schreck, C. Braeutigam, O. Konu, T. Brabletz, M.P. Stemmler, Enhancer cooperativity as a novel mechanism underlying the transcriptional regulation of E-cadherin during mesenchymal to epithelial transition, Biochim Biophys Acta, 1849 (2015) 731-742.

[76] B. Akhtar-Zaidi, R. Cowper-Sal-lari, O. Corradin, A. Saiakhova, C.F. Bartels, D. Balasubramanian, L. Myeroff, J. Lutterbaugh, A. Jarrar, M.F. Kalady, J. Willis, J.H. Moore, P.J. Tesar, T. Laframboise, S. Markowitz, M. Lupien, P.C. Scacheri, Epigenomic enhancer profiling defines a signature of colon cancer, Science, 336 (2012) 736-739.

[77] G.R. Diaferia, C. Balestrieri, E. Prosperini, P. Nicoli, P. Spaggiari, A. Zerbi, G. Natoli, Dissection of transcriptional and cis-regulatory control of differentiation in human pancreatic cancer, EMBO J, (2016).

[78] P.C. Taberlay, A.L. Statham, T.K. Kelly, S.J. Clark, P.A. Jones, Reconfiguration of nucleosome-depleted regions at distal regulatory elements accompanies DNA methylation of enhancers and insulators in cancer, Genome Res, 24 (2014) 1421-1432.

[79] R.P. Koche, Z.D. Smith, M. Adli, H. Gu, M. Ku, A. Gnirke, B.E. Bernstein, A. Meissner, Reprogramming factor expression initiates widespread targeted chromatin remodeling, Cell Stem Cell, 8 (2011) 96-105.

Figure legends

Fig. 1. Features of active chromatin at the *EPHB2* -8.4 kb enhancer are diminished upon expression of Snail1-HA. (A) Schematic representation of the human *EPHB2* upstream region from -12 kb to the transcriptional start site (TSS) and Exon 1 (Ex1). ECR: Evolutionarily conserved regions with sequence identities of more than 70% are shown by grey boxes. DHS: Clusters of DNaseI hypersensitivity in HUVEC cells. H3K4me1, H3K27ac: Levels of enrichment of the H3K4me1 and H3K27ac histone marks across the genome as determined by ChIP-seq assays in HUVEC cells. (B) FAIRE analyses of the *EPHB2* upstream region in LS174T cells stably transduced with Dox-inducible control and Snail1-HA retroviral expression vectors. Cells were treated with 0.1 µg ml^{-1} Dox for 144 h or were left untreated. A region 11 kb upstream of the *AXIN2* transcriptional start site served as negative control (- ctrl.). Data was calculated as relative enrichment of sequences of interest in formaldehyde-crosslinked versus non-crosslinked material. Shown are the mean and SEM; n = 3. *n.s.*: not significant. (C) ChIP analyses of H3, H3K4me1 and H3K27ac at positions -12.3 kb and -8.4 kb relative to the *EPHB2* transcriptional start site in LS174T cells stably transduced with Dox-inducible control and Snail1-HA retroviral expression vectors. Cells were treated with 0.1 µg ml^{-1} Dox for 0 h, 24 h and 96 h as indicated. Data was calculated as percent of input. In case of H3K4me1 and H3K27ac, enrichment was further normalized to H3 to account for regional differences in nucleosome density. Shown are the mean and SEM; n = 3.

Fig. 2. Mapping of an *EPHB2* minimal enhancer fragment with cell-type-specific activity. Luciferase reporter assays in four different CRC cell lines to narrow down the minimal cell-type-specific enhancer region within the *EPHB2* upstream region. The coordinates of the *EPHB2* enhancer subfragments are shown relative to the transcriptional start site. LUC: Luciferase coding sequence. SV40: SV40 promoter sequence. Shown are the mean and SEM; n = 3. *n.s.*: not significant.

Fig. 3. *EPHB2* enhancer activity depends on CDX2, TCF/LEF, MYB, and FOX proteins. (A) Nucleotide sequence of the *EPHB2* minimal enhancer region from -8398 bp to -8272 bp with binding sites for CDX2, TCF7L2, MYB and FOXA1 as predicted *in silico*. (B) Sequences of the predicted binding motifs for CDX2, TCF/LEF, MYB, and FOX proteins and the nucleotide exchanges introduced to abolish their binding. Mutated bases are shown in red. (C) EMSAs to analyze binding of recombinant CDX2, TCF7L2-E, MYB, and FOXA1 to the *EPHB2* minimal enhancer region *in vitro*. Note, that an E-type splice variant of TCF7L2 (TCF7L2-E) was used for the experiments [24]. Control samples received mock-programmed

transcription/translation mixes. Sequence changes in mutated probes are shown in (B). Non-specific signals are labeled with asterisks. For each transcription factor one representative EMSA experiment is shown; n = 3. WT: wild-type; MUT: mutated. (D) Luciferase reporter assays in LS174T cells to identify functionally important transcription factor binding sites within the *EPHB2* minimal enhancer region. Sequence changes in mutated (mut) probes are depicted in (B). Results shown are the mean and SEM; n = 3.

Fig. 4. Snail1 inactivates the *EPHB2* -8.4 kb enhancer by downregulation of FOXA1 and MYB. (A) qRT-PCR analyses of *Snail1-HA*, *CDX2*, *FOXA1*, and *MYB* expression relative to *GAPDH* (rel. expr.) in LS174T cells stably transduced with Dox-inducible control and Snail1-HA retroviral expression vectors. Cells were treated with 0.1 µg ml^{-1} Dox for the indicated time periods. Shown are the mean and SEM; n = 3. (B) Western blot analyses of CDX2, FOXA1, and MYB in LS174T cells stably transduced with Dox-inducible control and Snail1-HA retroviral expression vectors. RNA Polymerase II (POL2) immunodetection served as loading control. One representative example is shown; n = 3. (C) Pairwise correlation analyses of *EPHB2*, *CDX2*, *MYB*, *FOXA1*, *TCF7L2*, *SNAI1*, *SNAI2*, and *ZEB1* expression in 290 colorectal tumor samples (left) and 155 CRC cell lines (right). The red/blue color shading indicates the Pearson correlation coefficient as shown by the color bar. (D) ChIP analyses of MYB, FOXA1, and CDX2 at positions -12.3 kb and -8.4 kb relative to the *EPHB2* transcriptional start site in LS174T cells stably transduced with Dox-inducible control and Snail1-HA retroviral expression vectors. Cells were treated with 0.1 µg ml^{-1} Dox for the indicated time periods. Data was calculated as percent of input. Shown are the mean and SEM; n = 3. *n.s.*: not significant.

Fig. 5. Snail1 overexpression induces a TCF7L2/LEF1 switch at the *EPHB2* -8.4 kb enhancer. (A) qRT-PCR analyses of LEF1 and TCF7L2 expression relative to GAPDH (rel. expr.) in LS174T cells stably transduced with Dox-inducible control and Snail1-HA retroviral expression vectors. Cells were treated with 0.1 µg ml^{-1} Dox for the indicated time periods. Shown are the mean and SEM; n = 3. (B) Western blot analyses of LEF1 and TCF7L2 expression in LS174T cells stably transduced with Dox-inducible control and Snail1-HA retroviral expression vectors. The positions of TCF7L2-E and TCF7L2-M/S splice variants are shown. Cells were treated with 0.1 µg ml^{-1} Dox for the indicated time periods. Immunodetection of α-TUBULIN (TUB) served as loading control. One representative example is shown; n = 3. (C) Competitive EMSA to compare affinity of LEF1 and TCF7L2-E for the TCF/LEF motif within the *EPHB2* minimal enhancer region *in vitro*. Nucleotide sequences of wild-type and mutated probes are shown. The TCF/LEF binding motif is highlighted by bold letters and nucleotide exchanges are indicated in red. Western blot

36

analysis of *in vitro* translated (IVT) TCF7L2-E and LEF1 proteins (left) and one representative example for the EMSA results (right) are shown; n = 3. Non-specific signals in the EMSA are labeled with asterisks. (D) ChIP analyses of TCF7L2 and LEF1 at positions 12.3 kb and -8.4 kb relative to the *EPHB2* TSS in LS174T cells stably transduced with Dox-inducible control and Snail1-HA retroviral expression vectors. Cells were treated with 0.1 µg ml^{-1} Dox for the indicated time periods. Data was calculated as percent of input. Shown are the mean and SEM; n = 3.

Fig. 6. Overexpression of Lef1-HA is not sufficient to permanently downregulate *EPHB2*. (A) qRT-PCR analyses of *Lef1-HA*, *EPHB2*, *SNAI1*, *FOXA1*, *MYB* and *CDX2* expression relative to *GAPDH* (rel. expr.) in LS174T cells stably transduced with Dox-inducible control and Lef1-HA retroviral expression vectors. Cells were treated with 0.1 µg ml^{-1} Dox for the indicated time periods. Shown are the mean and SEM. n = 3. *n.s.*: not significant. (B) Western blot analyses of EPHB2, Lef1-HA, CDX2, FOXA1 and MYB expression in LS174T cells stably transduced with Dox-inducible control and Lef1-HA retroviral expression vectors. Cells were treated with 0.1 µg ml^{-1} Dox for the indicated time periods. TUB and POL2 immunodetection served as loading controls. Whole cell lysates and nuclear extracts were used for the experiments shown in the left and right parts of the panel, respectively. One representative example is shown; n = 3. (C) ChIP analyses of Lef1-HA and TCF7L2 at *EPHB2* -12.3 kb and -8.4 kb in LS174T cells, stably transduced with Dox-inducible control and Lef1-HA retroviral expression vectors, treated with 1.0 µg ml^{-1} Dox for the indicated time periods. Data was calculated as percent of input. Shown are the mean and SEM; n = 3. (D) ChIP analyses of FOXA1, MYB and CDX2 at *EPHB2* -12.3 kb and -8.4 kb in LS174T cells, stably transduced with Dox-inducible control and Lef1-HA retroviral expression vectors, treated with 0.1 µg ml^{-1} Dox for the indicated time periods. Data was calculated as percent of input. Shown are the mean and SEM; n = 3. *n.s.*: not significant. (E) Model for Snail1-mediated silencing of *EPHB2* expression through inactivation of the *EPHB2* enhancer by competitive displacement and deprivation of its constituent transcriptional activators.
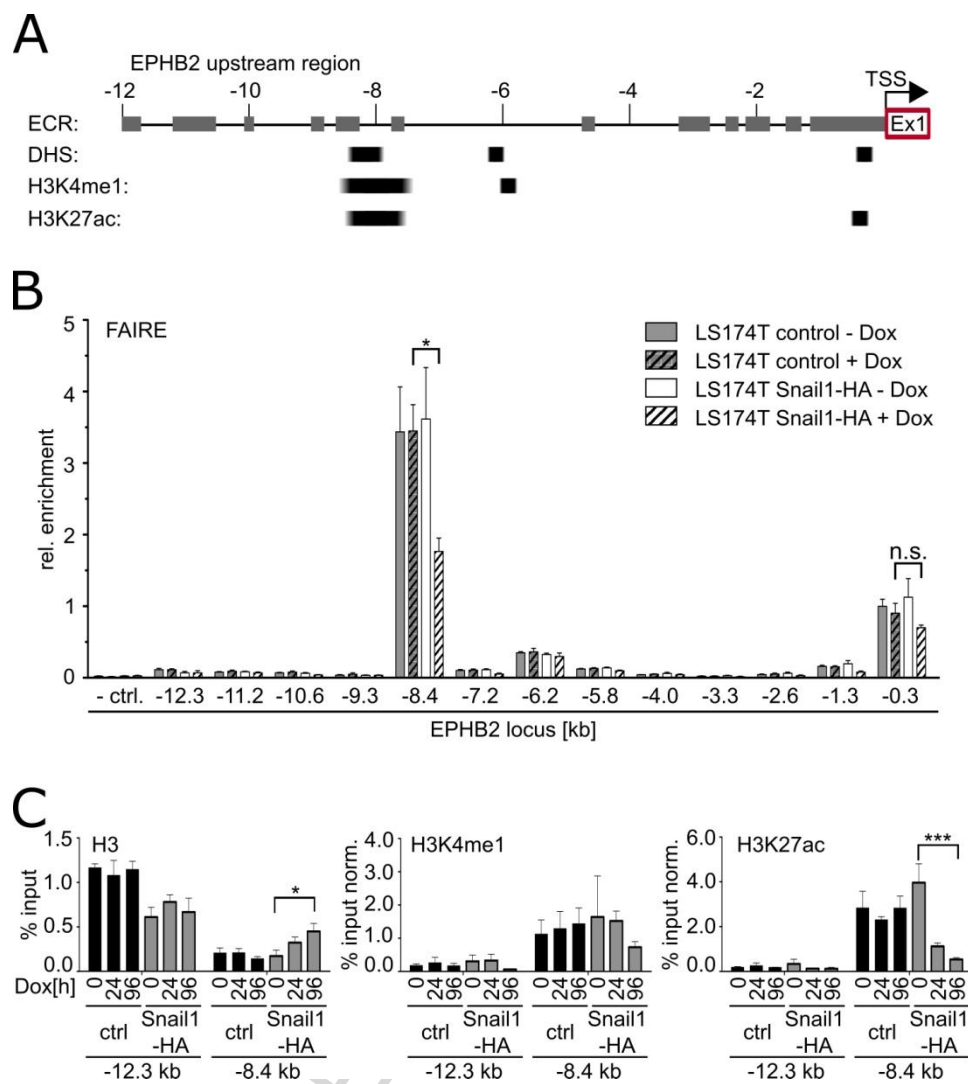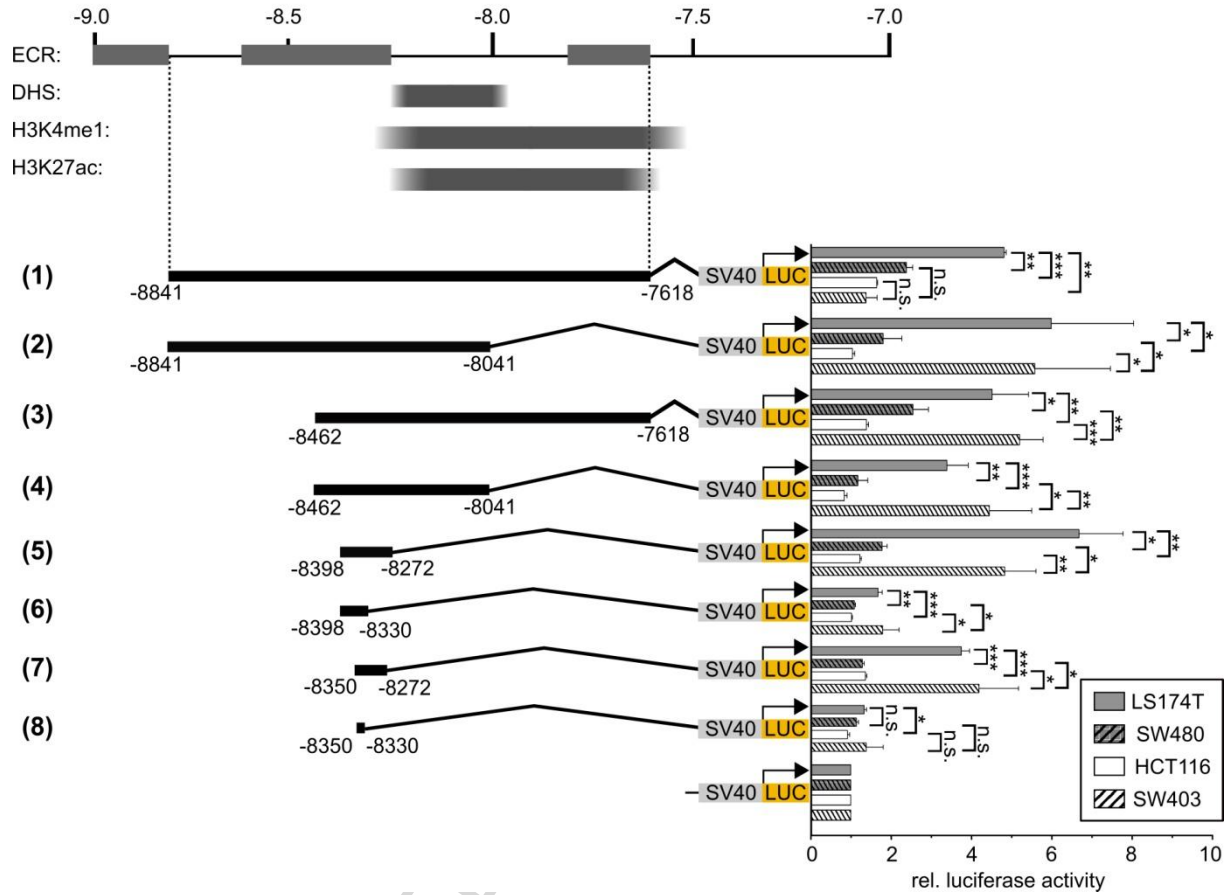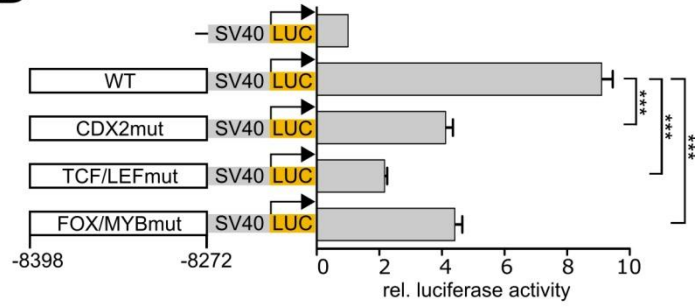
37

Figure 1

Figure 2

A

GGTCGGCCAGGGGAATAGCCATAAAATTCTGTGTGCTCCTGTGGGGCGCAAAGATCAAAGTATCCCATATCAGTCTCAGTATACAACCGTAACAACATAACAACCTTTTACCTGGATACGGCACTCC

-8398

CDX2 TCF/LEF FOX / MYB

-8272

B

Mutations:

CDX2:	ATAAAA	→ A**GCCG**A
TCF/LEF:	AGATCAAAG	→ **TGGC**CAAAG
FOX:	ACAACC	→ AC**CCC**C
MYB:	AACCG	→ **CC**CCG

D

	SV40 **LUC**	
WT	SV40 **LUC**	
CDX2mut	SV40 **LUC**	
TCF/LEFmut	SV40 **LUC**	
FOX/MYBmut	SV40 **LUC**	

-8398 -8272

rel. luciferase activity

***

C

Lanes 1 2 3 4

*
CDX2 →
CDX2 →
Probe WT mut WT mut
CDX2 − − + +

*
*
TCF7L2-E →
Probe WT mut WT mut
TCF7L2-E − − + +

*
*
FOXA1 →
FOXA1 →
Probe WT mut WT mut
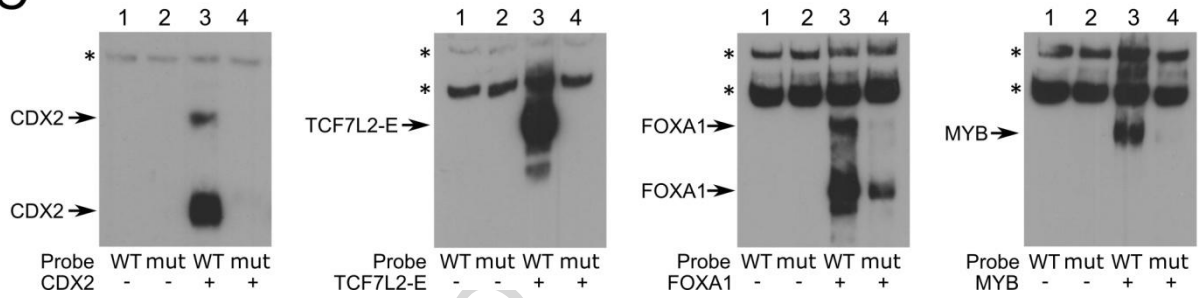FOXA1 − − + +

*
*
MYB →
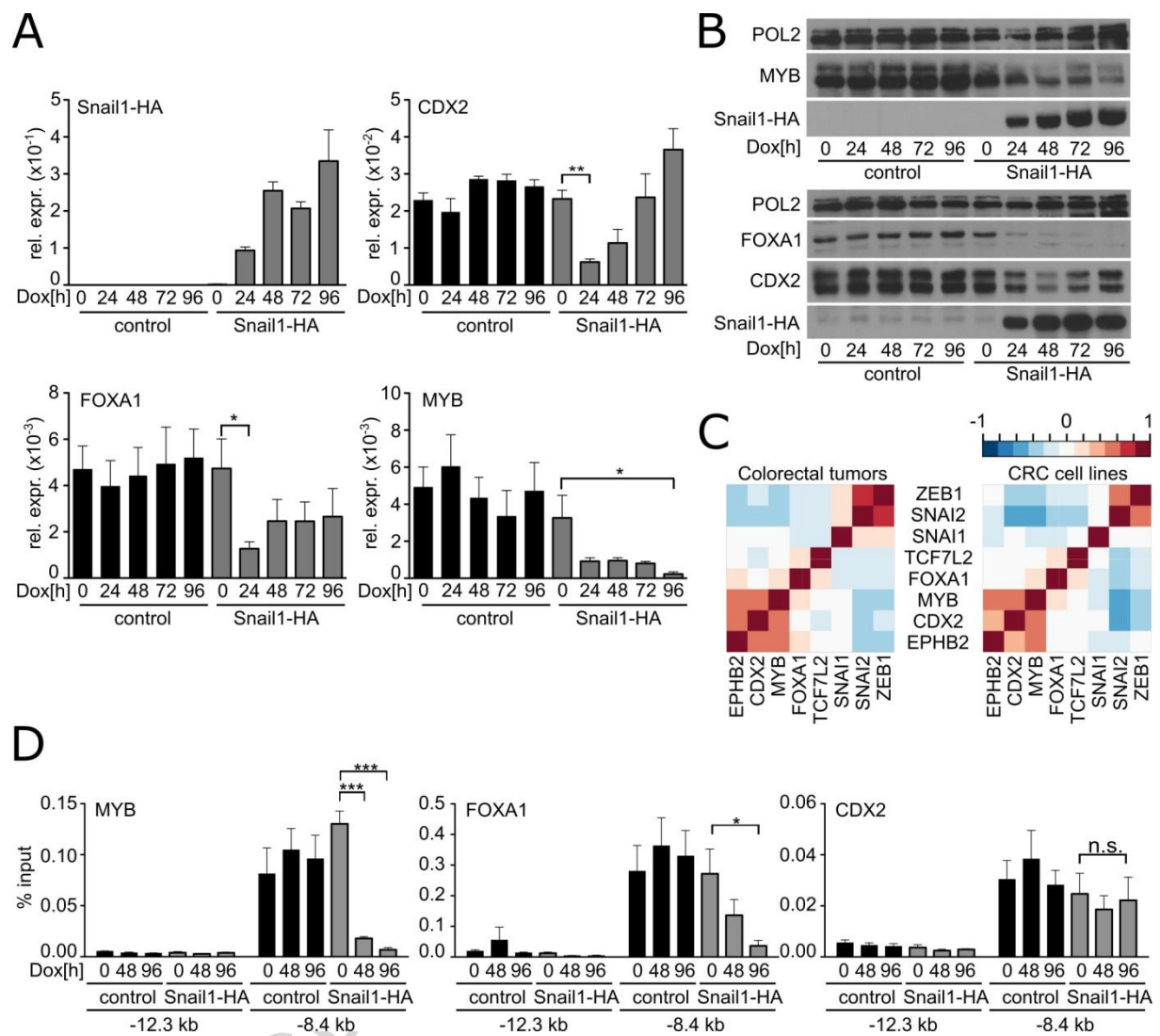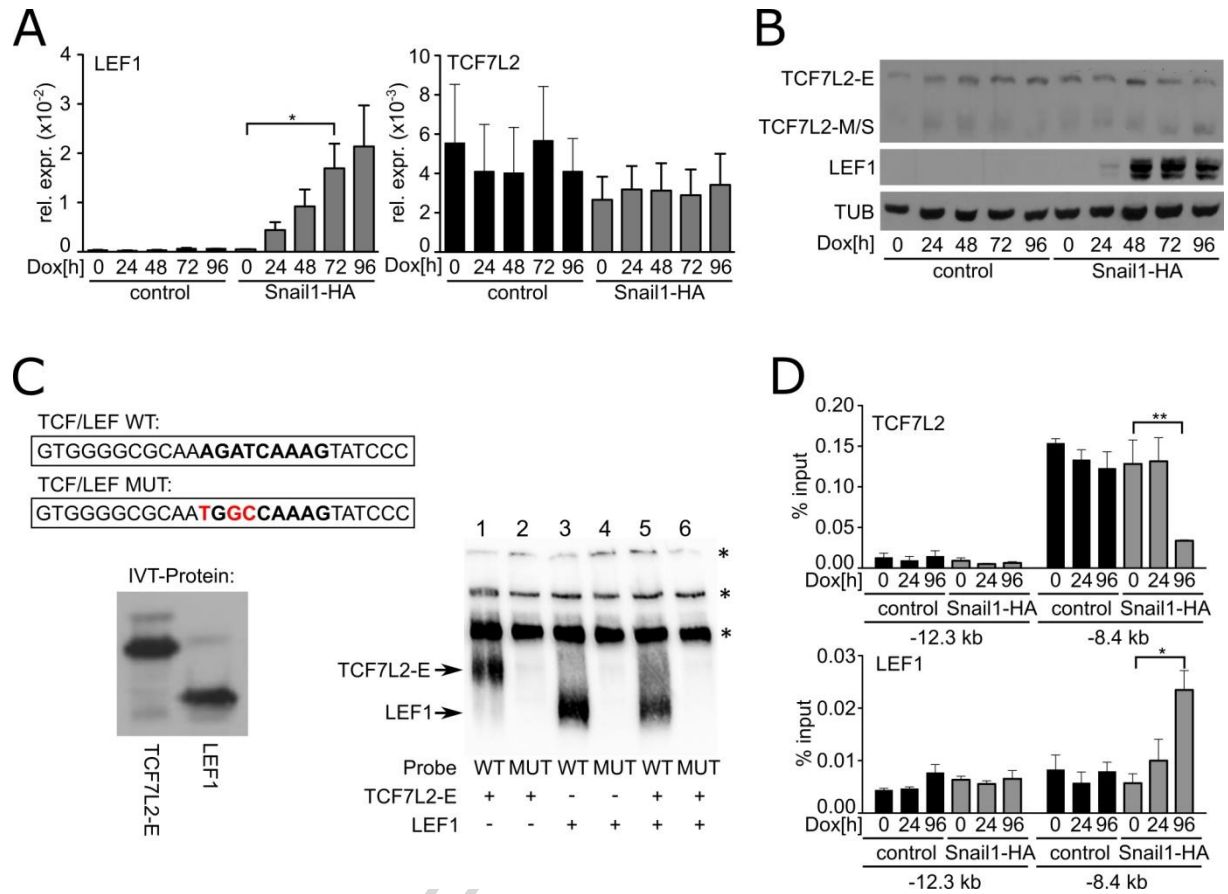Probe WT mut WT mut
MYB − − + +

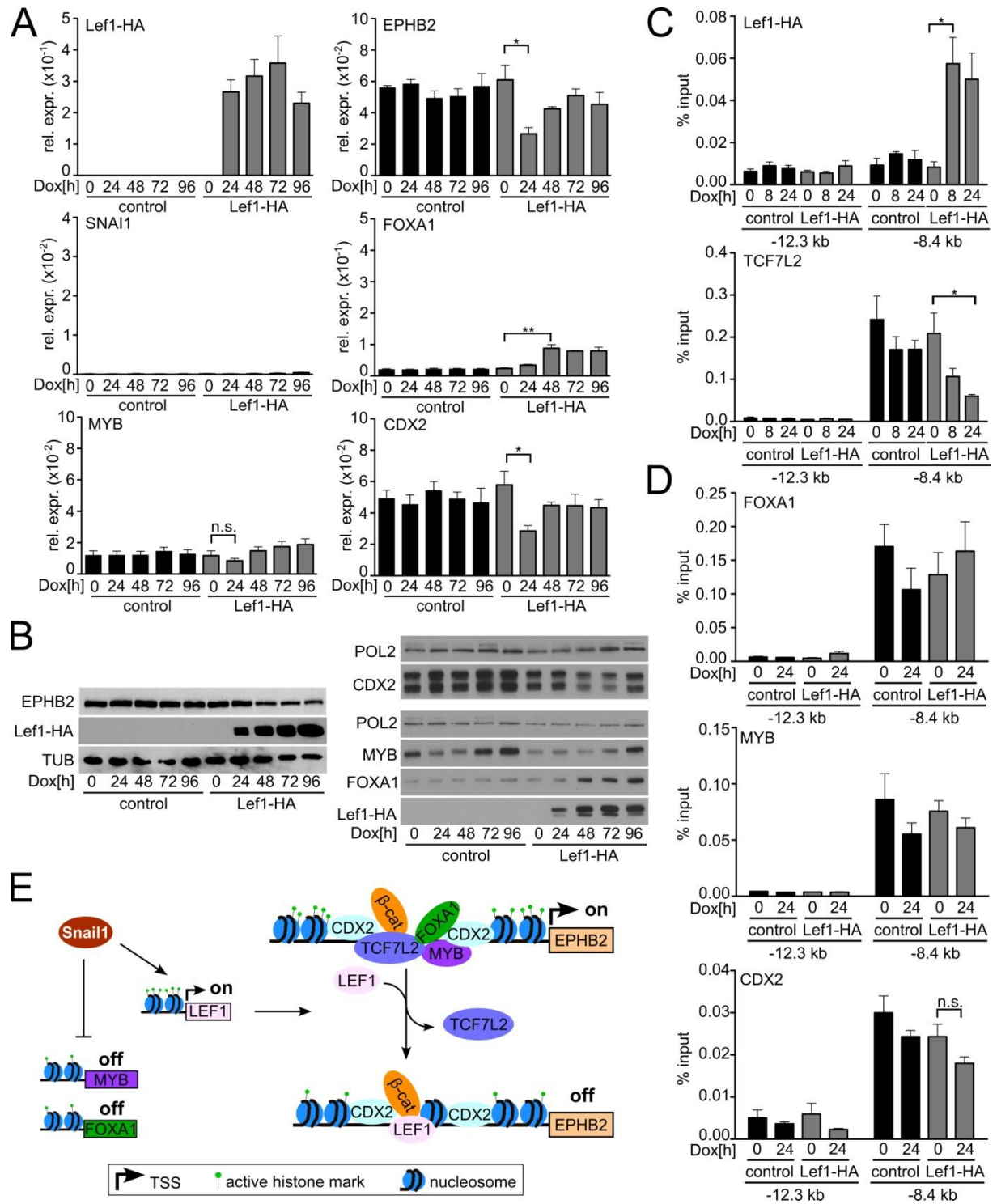Figure 3

Figure 4

Figure 5

Figure 6

Table 1: Sequences of oligonucleotides used for PCR, mutagenesis, quantitative RT-PCR, EMSA, FAIRE and ChIP

Oligonucleotides for PCR:

Primer:	Forward (5'-3')	Reverse (5'-3')
EPHB2 -8841/-7618	TCACGCGTAGAAGCCTGCCTGCTTATCA	CTGCTAGCCCTGACACATGGGCACTGAC
EPHB2 -8841/-8041	TCACGCGTAGAAGCCTGCCTGCTTATCA	CTGCTAGCGTCTCCCAATTCCCCAGATT
EPHB2 -8462/-7618	TCACGCGTGCACCTCTGTTACCAGGAACC	CTGCTAGCCCTGACACATGGGCACTGAC
EPHB2 -8462/-8041	TCACGCGTGCACCTCTGTTACCAGGAACC	CTGCTAGCGTCTCCCAATTCCCCAGATT
EPHB2 -8398/-8272	TCACGCGTGGTCGGCCAGGGGAATAGCC	CTGCTAGCGGAGTGCCGATCCAGGTAAAAG
EPHB2 -8398/-8330	GGTCGGCCAGGGGAATAGCCATAAAATTCTGTGTGCTCCTGTGGGGCGCAAAGATCAAAGTATCCCATG	CTAGCATGGGATACTTTGATCTTTGCGCCCCACAGGAGCACACAGAATTTTATGGCTATTCCCCTGGCCGACCGAGCT
EPHB2 -8350/-8272	CCAAAGATCAAAGTATCCCATATCAGTCTCAGTATACAACCGTAACAACATAACAACCTTTTACCTGGATACGGCACTCCG	CTAGCGGAGTGCCGTATCCAGGTAAAAGGTTGTTATGTTGTTACGGTTGTATACTGAGACTGATATGGGATACTTTGATCTTTGGAGCT
EPHB2 -8350/-8330	CCAAAGATCAAAGTATCCCATG	CTAGCATGGGATACTTTGATCTTTGGAGCT
EPHB2 -11073/-10237	TCACGCGTAAAATGGCGAGAACAACCAG	CTGCTAGCGACATGAGCCACCATACACG
EPHB2 -6453/-5951	GAACGCGTAAGAGGTGGTGCTGGATTTG	CTGCTAGCGTGATGGGCCGTGAAACCAG

Oligonucleotides for mutagenesis (mutated bases underlined):

Primer:	Forward (5'-3')	Reverse (5'-3')
CDX2	CGGCCAGGGGAATAGCCA<u>GCCG</u>ATTCTGTGTGCTCCTGTGGGG	CCCCACAGGAGCACACAGAAT<u>CGGC</u>TGGCTATTCCCCTGGCCG
TCF/LEF	GCTCCTGTGGGGCGCAA<u>TGGC</u>CAAAGTATCCCATATC	GATATGGGATACTTT<u>GGCC</u>ATTGCGCCCCACAGGAG
FOX/MYB	TCCCATATCAGTCTCAGTATAC<u>CC</u>CCGTAACAACATAACAAC	GTTGTTATGTTGTTACGG<u>GGG</u>TATACTGAGACTGATATGGGA

Oligonucleotides for quantitative RT-PCR:

Primer:	Forward (5'-3')	Reverse (5'-3')
EPHB2	AGTTCGGCCAAATTGTCAAC	TCTCCTTGTACTGCCCCATC
Lef1-HA	TATGAACAGCGACCCGTACA	TCGTCGCTGTAGGTGATGAG

	Forward	Reverse
LEF1	CGAATGTCGTTGCTGAGTGT	GCAGACCAGCCTGGATAAAG
Snail1-HA	CTTGTGTCTGCACGACCTGT	CTTCACATCCGAGTGGGTTT
SNAI1	TTTACCTTCCAGCAGCCCTA	CCTCATCTGACAGGGAGGTC
TCF7L2	TGCGTTCGCTACATACAAGG	TGGGTCTGCTCAGTCTGTGA
CDX2	CCCGAACAGGGACTTGTTTA	AGACCAACAACCCAAACAGC
MYB	ACAGATGGGCAGAAATCGCA	GCTGGCTGGCTTTTGAAGAC
FOXA1	AGCAGCAGCATAAGCTGGAC	GTGTTTAGGACGGGTCTGGA
SNAI2	GAGCATTTGCAGACAGGTCA	GCTTCGGAGTGAAGAAATGC
SNAIL2-HA	GAGCATTTGCAGACAGGTCA	GGACGTCATAAGGATATCCAGCA
ZEB1	CCTTAAGCAAGACCTGTGTGC	CCGAGGAATTGAAGGATGAA
ZEB1-HA	CACCAAGTGCCAACCCCATA	CAGGGCTGACCGTAGTTGAG
BMP2	GTCCCGACAGAACTCAGTGC	TCAACTGGGGTGGGGTTTTT
BMP4	TGTTGTGTGCCCACTGAACT	TGAGTGGATGGGAACGTGTG

Oligonucleotides for EMSA (biotinylated):

Primer:	Forward (5'-3')	Reverse (5'-3')
EPHB2 -8398/-8272	TCACGCGTGGTCGGCCAGGGGAATAGCC	CTGCTAGCGGAGTGCCGTATCCAGGTAAAG

Oligonucleotides for FAIRE and ChIP:

Primer:	Forward (5'-3')	Reverse (5'-3')
AXIN2	TTGACCTCGGGAATCTGTTC	CCATCCCCACCTTCTCTTCT
EPHB2 -12.3	GGTGGGAGGACAACAGACAC	CTACAGCAGGAGCTGGGAAC
EPHB2 -11.2	ATGCATGCGGAGCTTAAAAC	TGGCAGTTGGAAGAATCCTG
EPHB2 -10.6	TCCACCTCAGACAGTTGCAG	GACATGAGCCACCATACACG
EPHB2 -9.3	AGAGAATTTGGGGCAGTGAA	AGGTTGAGGCTGCAGTGAGT
EPHB2 -8.4	CAGGAGAGACGCAGATTG	AAGGTTGTTATGTTGTTACGG
EPHB2 -7.2	TGAAGTTTGAGGCTGCAATG	GCCTTTGGAGTTAGGGAAGG
EPHB2 -6.2	AGGGGTCAAAAGTGGAAACC	TGTGACTCAGAGCTGGAGGA
EPHB2 -5.8	AACCCAAGGGAATGCTCACT	AATCTCCACAGCCTGAGAGC
EPHB2 -4.0	CTGGCTGTAGGGATGGTTTG	GGGGGAAACATGTTACACTGA
EPHB2 -3.3	CCCTGATGTAACCTCCTCCA	ATCAGGGAAGGCCTCTTAGG
EPHB2 -2.6	CTTAAACCGCCTCCTCCTCT	ACATGGTCCATTGCTGGTTT
EPHB2 -1.3	CTCCCTGCTCACTCCTGTTC	TACCACAGGCTTTGGGAATC
EPHB2 -0.3	GGCTTTGCAGCATTCAATAA	CGCAGCAGTGGTCTCTCC

Highlights

- Epithelial-mesenchymal transition leads to repression of *EPHB2* in colorectal cancer

- *EPHB2* expression depends on a transcriptional enhancer

- FOXA1, MYB, CDX2 and the Wnt pathway effector TCF7L2 are *EPHB2* enhancer factors

- SNAIL1-induced expulsion of TCF7L2 by repressive LEF1 impairs *EPHB2* enhancer activity

- SNAIL1 represses FOXA1 and MYB for further activator deprivation of the enhancer